Search for Randall-Sundrum Gravitons in the di-Electron & di-Photon Channel at DØ

Ning Zhou
Columbia University

FNAL 2009-12-01

Outline

1. Motivation

   Hierarchy Problem and Randall-Sundrum Model

2. Experiment and Data

   DØ RunII data @ Tevatron

3. Search Strategy

   di-Electron and di-Photon Channel

4. Results

   The results with the full dataset are currently undergoing DØ internal review. For this talk, signal region of RunIIa data only is shown here.

5. Outlook

Motivation

- Hierarchy Problem - The large disparity between the Planck Scale (10^{16} TeV) and the electroweak symmetry breaking scale (~1TeV)
- Possible explanations: SUSY, Extra Dimensions, etc.
- Take the Randall-Sundrum Extra Dimension Model

5 dimensional warped geometry

$$ds^2 = e^{-2\sigma(\phi)}\eta_{\mu\nu}dx^\mu dx^\nu + r_c^2 d\phi^2$$

metric

$$\sigma(\phi) = kr_c|\phi|$$

warp factor

r_c : compactification of the extra dimension
ϕ : the 5th coordinate, $0 < |\phi| < \pi$
k : 5th dimension curvature scale of order the Planck Scale.

Randall-Sundrum Model

- Gravitybrane $\phi = 0$ and Weakbrane $\phi = \pi$
- SM fields: Weakbrane.
- Graviton: Gravitybrane, the only particle propagating in the 5th dimension.

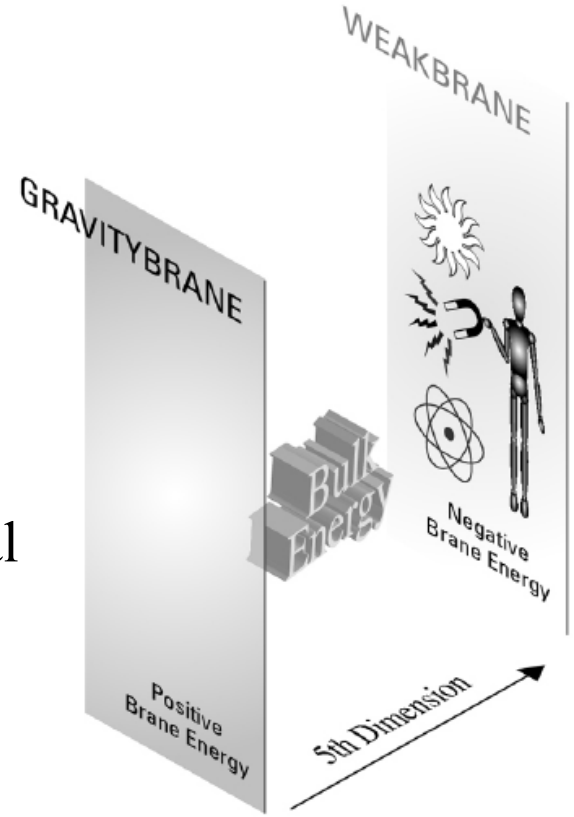

- Any mass parameter M on the Weakbrane will correspond to a physical mass M_0 in the fundamental higher dimensional theory.

$$M = \exp(-kr_c\pi)M_0$$

TeV scales are generated from fundamental scales of order M_{Pl} via a geometrical exponential factor if $kr_c \sim 11\text{-}12$.

Kaluza-Klein Gravitons

- Compactification of 5th dimension : Kaluza-Klein tower
- Kaluza-Klein graviton modes :

  $m_n = kx_n \exp(-kr_c\pi) = x_n(k/\overline{M}_{Pl})\Lambda_\pi$ where $J_1(x_n)=0$, $\Lambda_\pi \sim$ TeV
- Spin-2
- First excitation : only decays into SM states

  with coupling strength ~ 1/TeV
- Parameters : 1) First excitation mass m_1

  2) coupling constant $k/\overline{M}_{Pl}$

  $k/\overline{M}_{Pl} \leq 0.1$ <= perturbative theory

  $0.01 \leq k/\overline{M}_{Pl}$ <= no new hierarchy issue

Graviton Production and di-EM Decay Channel

BR(γγ) / BR(ee) = 2

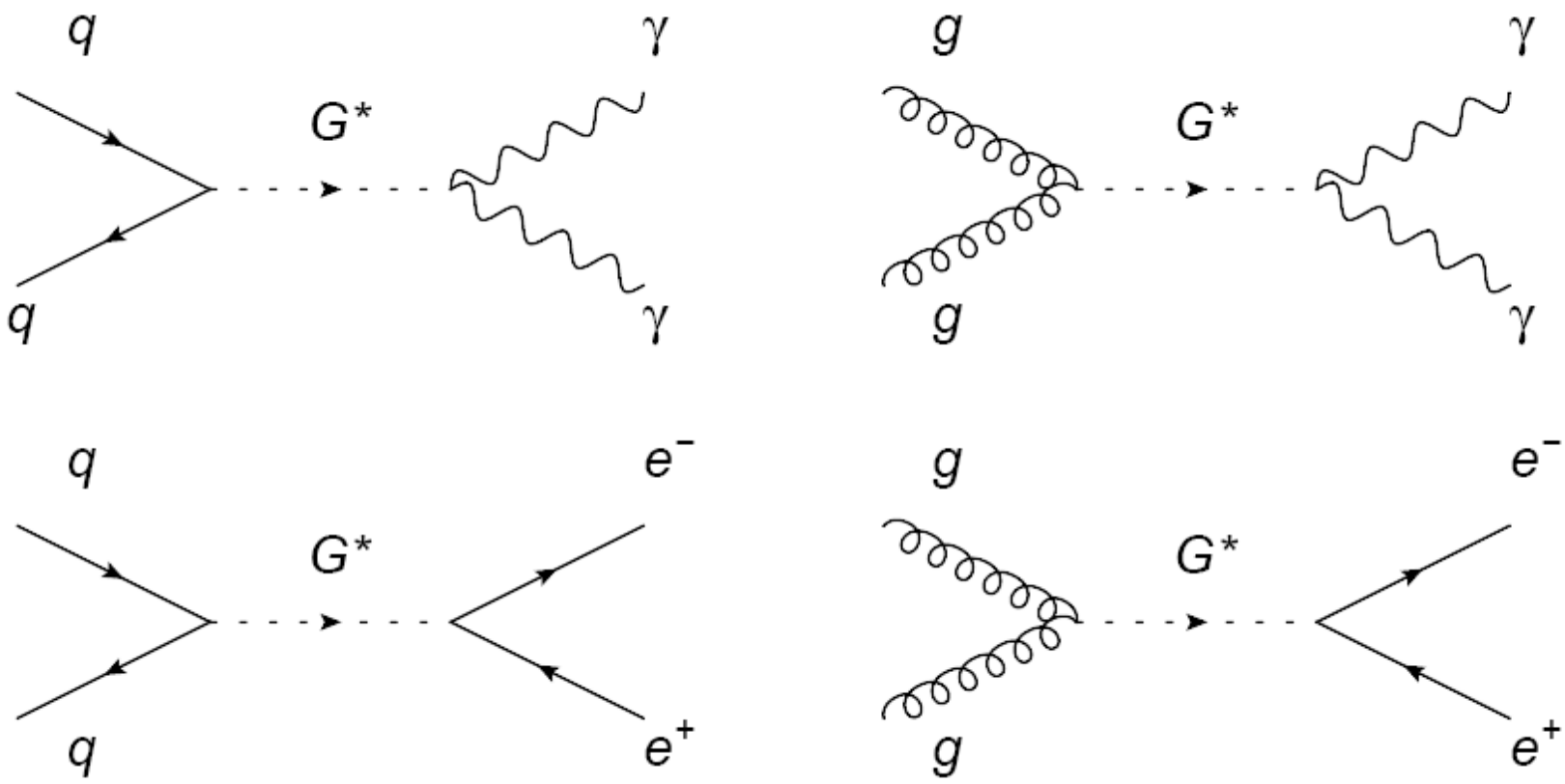

Graviton at Tevatron

narrow resonance for coupling constant less than 0.1

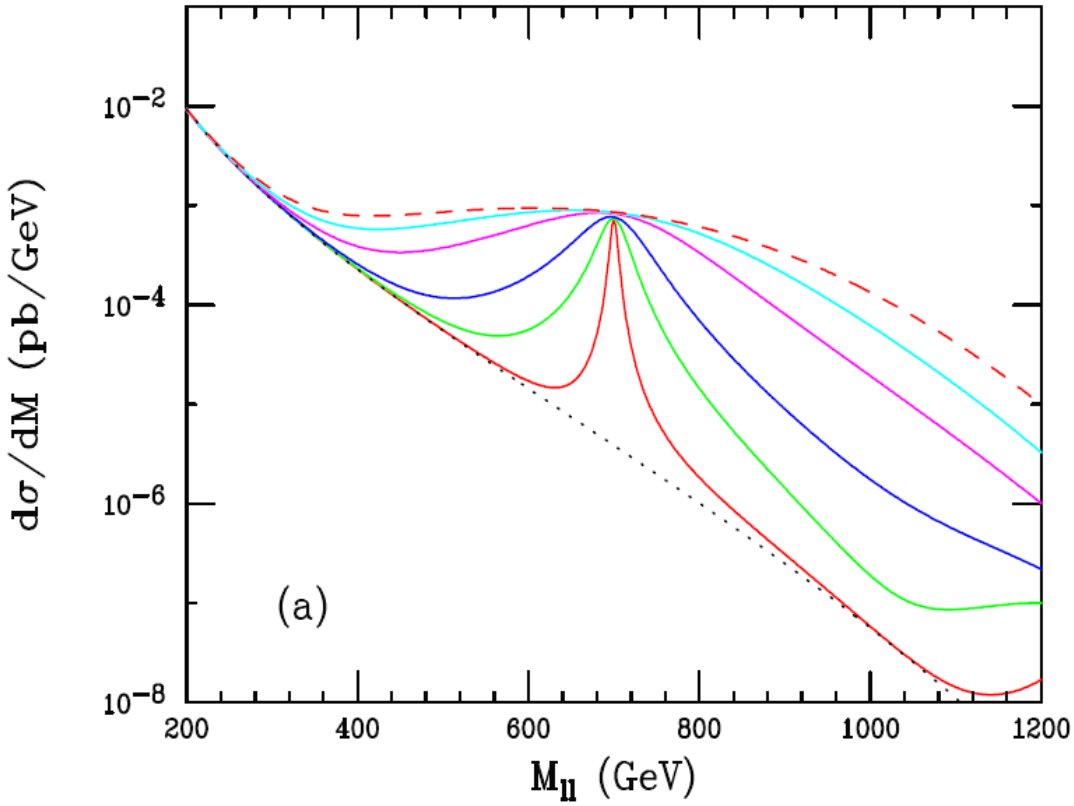

Drell-Yan production of 700GeV Kaluza-Klein graviton at the Tevatron with coupling constant 1, 0.7, 0.5, 0.3 and 0.1, from top to bottom.

(*PRD*, ***63***, *075004*)

Published Search Results

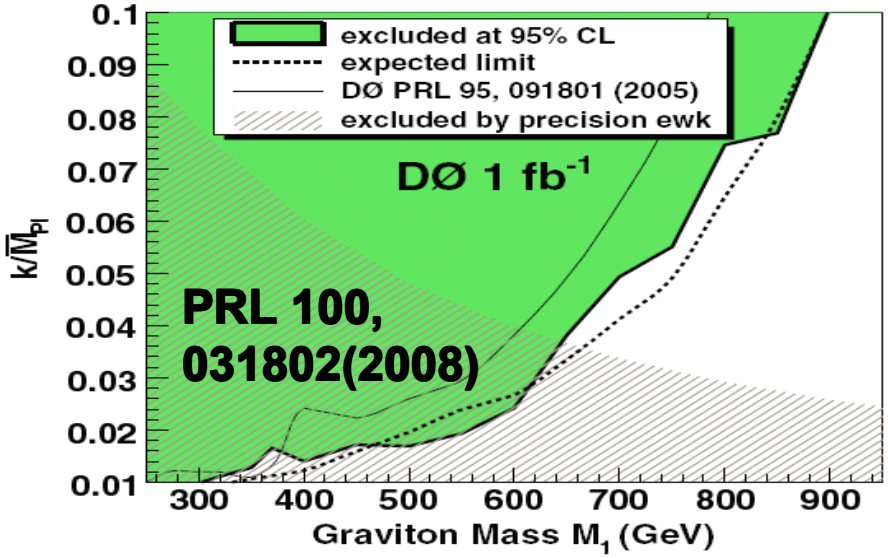

ee+γγ channel 1fb^{-1}

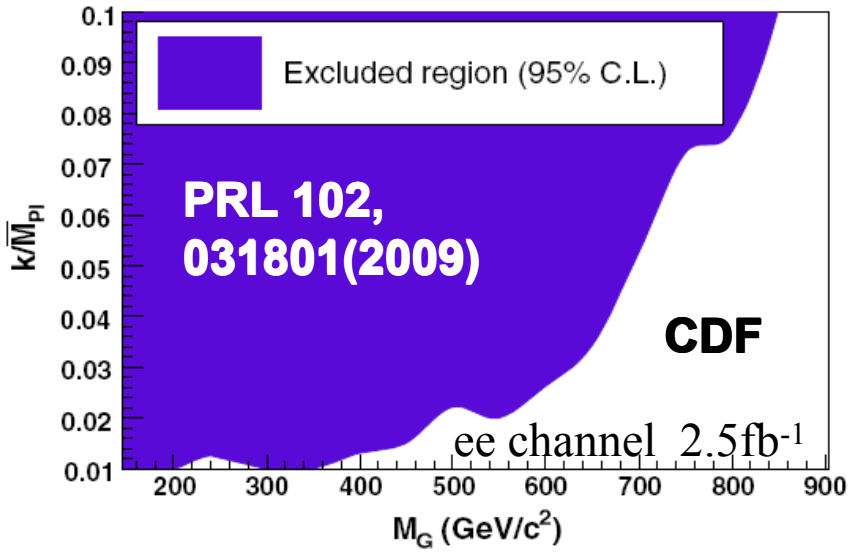

RS graviton with mass below 200GeV is excluded at 95% confidence level for coupling constant larger than 0.01.

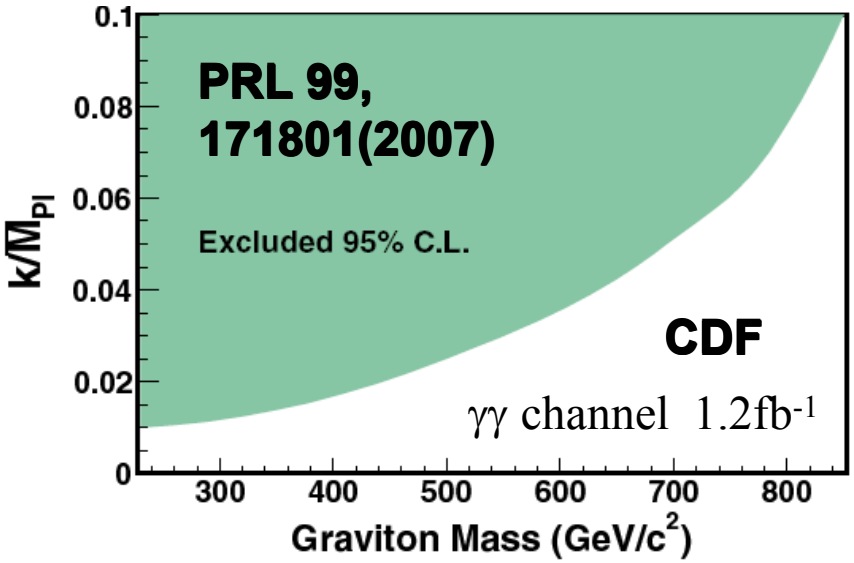

Tevatron @ FNAL

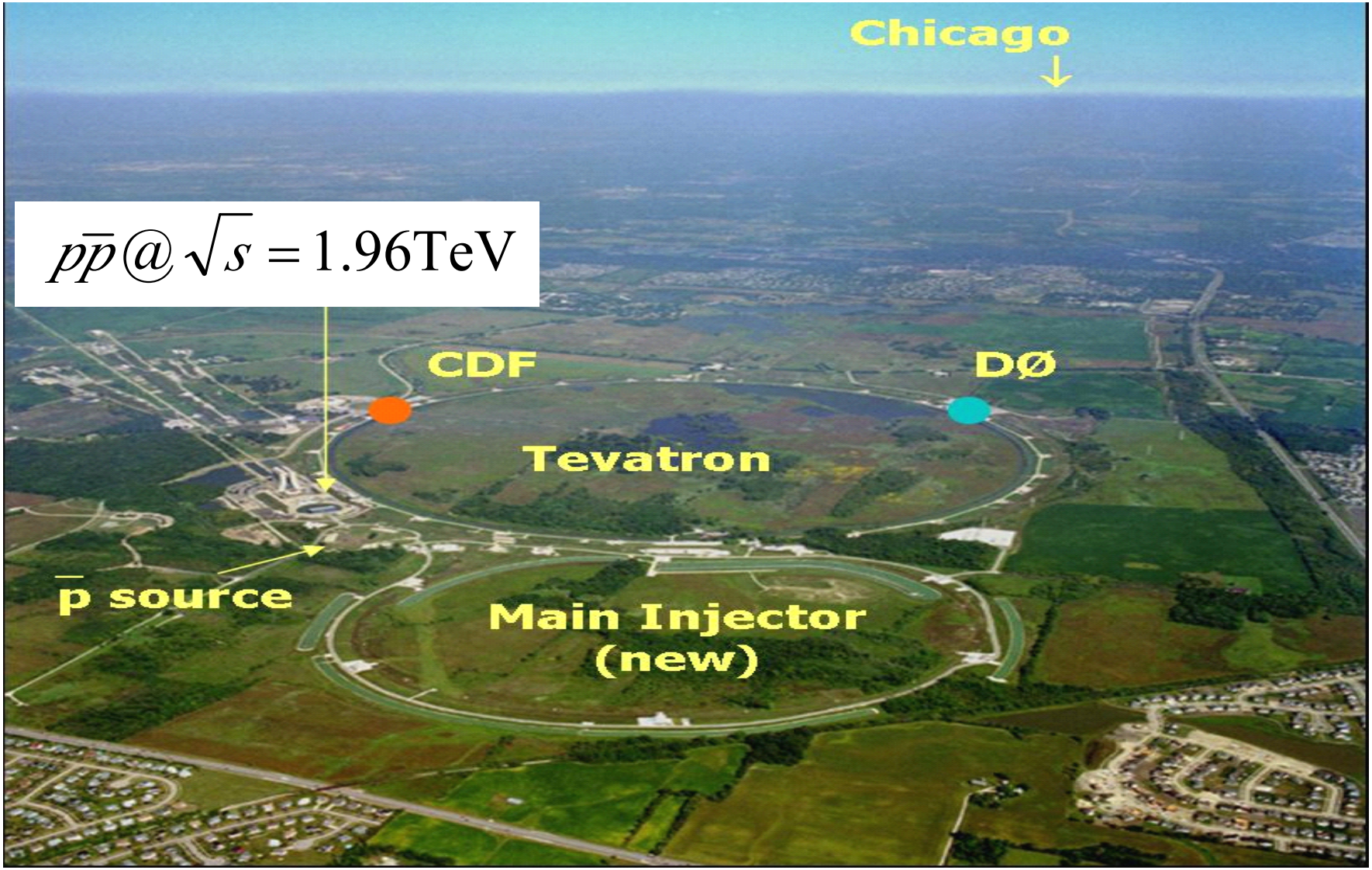

DØ Experiment

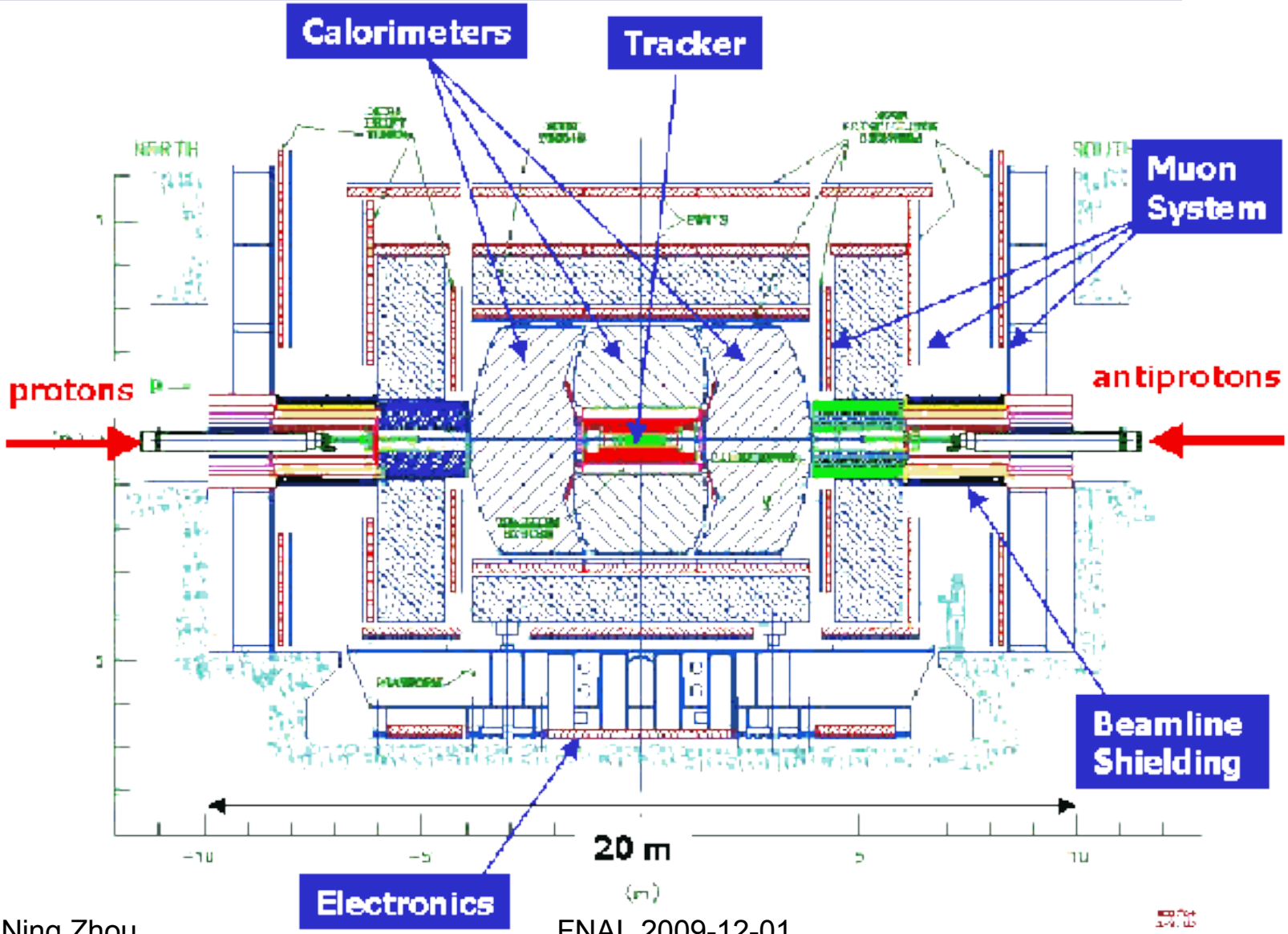

Track, Preshower and Calorimeter

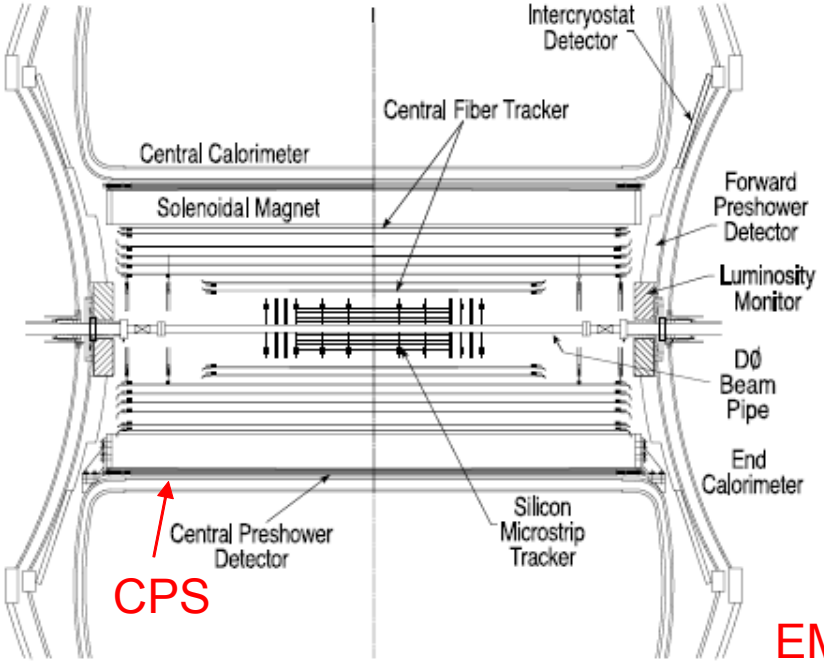

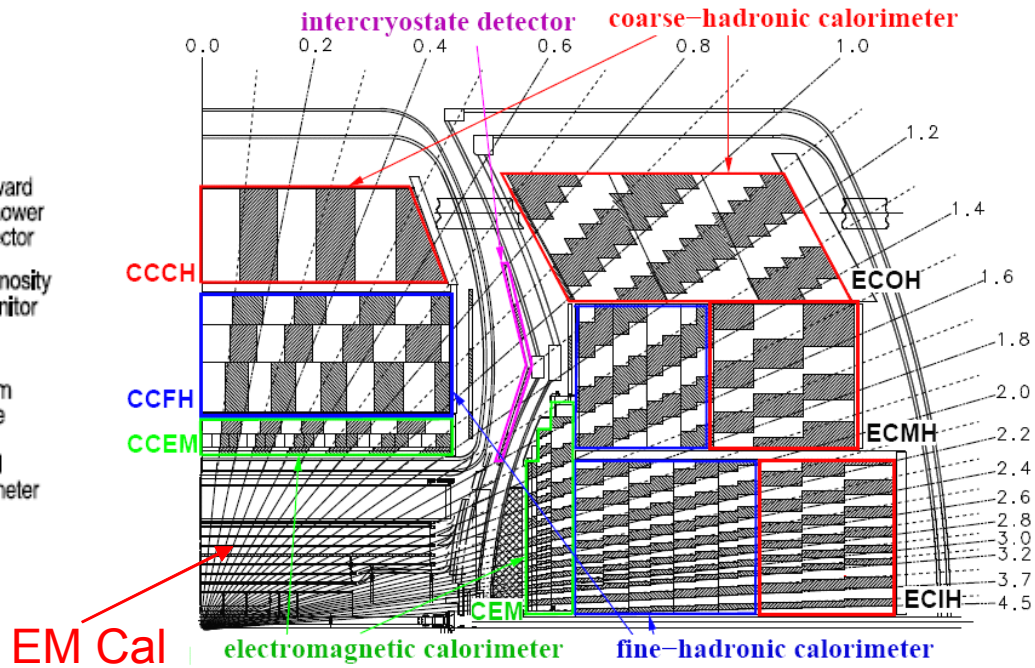

Overview of DØ tracking, preshower and calorimeter systems.

- Electrons or photons are reconstructed from EM clusters in calorimeter with or without tracks associated.
- Central preshower cluster matched to EM shower can be used to point back to the production vertex, with resolution along the z-axis of ~3.6cm.

Luminosity

The dataset used in this analysis is collected at DØ from 07/2002 until 06/2009

=> $5.4 fb^{-1}$

1) RunIIa (before 02/2006) $1.1 fb^{-1}$ 2) RunIIb (after 06/2006) $4.3 fb^{-1}$

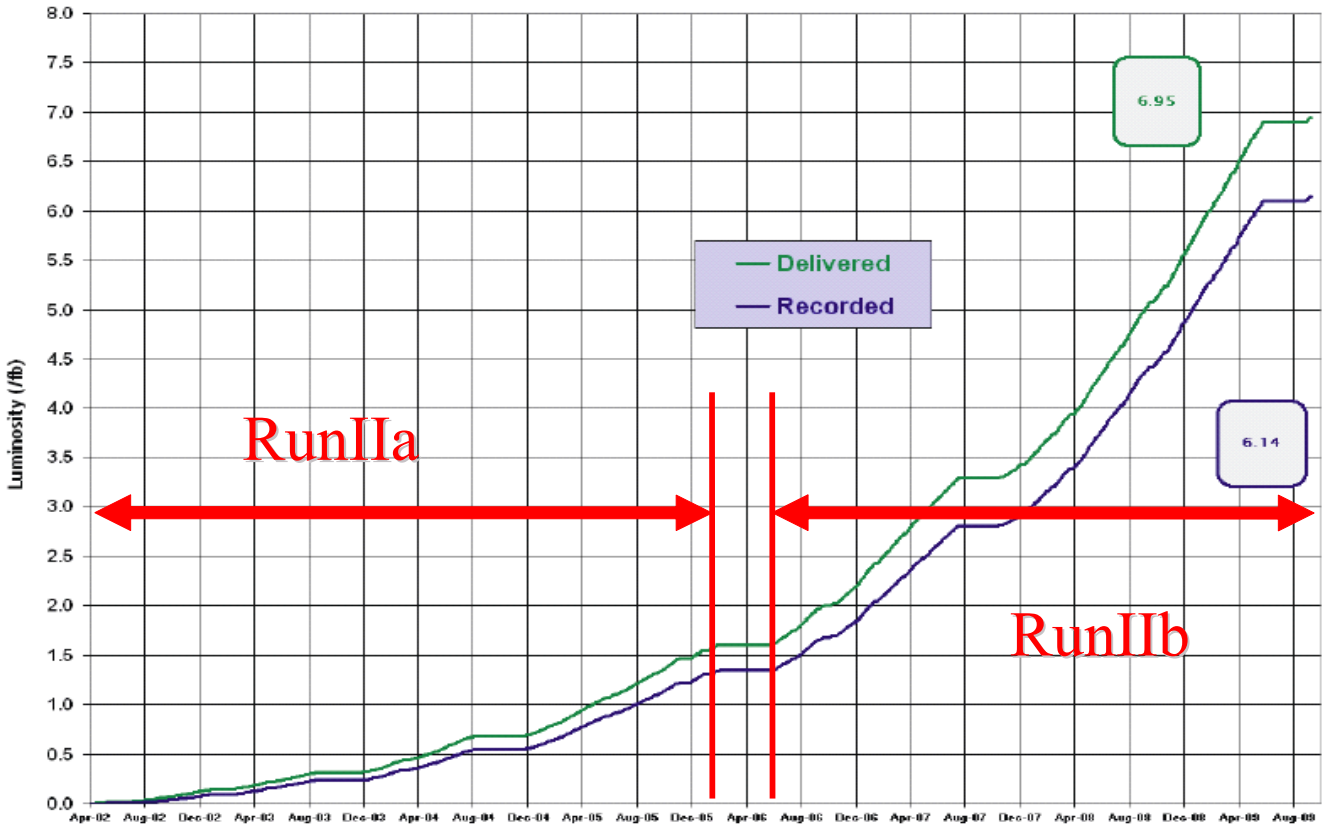

Search Strategy

Graviton Signal:

- A narrow resonance in the di-EM invariant mass spectrum.
- BR($\gamma\gamma$)/BR(ee) = 2

Split the data into two non-overlapping categories ("di-electron" and "di-photon") to optimize the sensitivity, based on tracking information.

Category I : "di-electron"

events with both EM objects passing track match requirements

Category II : "di-photon"

events with at least one object failing the track requirements

Search Strategy (cont'd)

SM Background:

- spectrum: Determine the invariant mass shape for each SM background.
- normalization:

  Derive each background's contribution in the data by fitting the data mass spectrum in the Control Region with invariant mass below 200GeV.

  Normalize the background shapes to their contributions in the data

- extrapolation : Extrapolate background model from fit into the Signal Region with invariant mass above 200GeV.

Signal Search:

Compare the spectra of background only (B) and signal plus background (S+B) with that of data in the signal region.

Graviton Signals

G->ee , *G->γγ* : PYTHIA

NLO correction gives a k-factor of 1.54 *hep-ph/0506158*

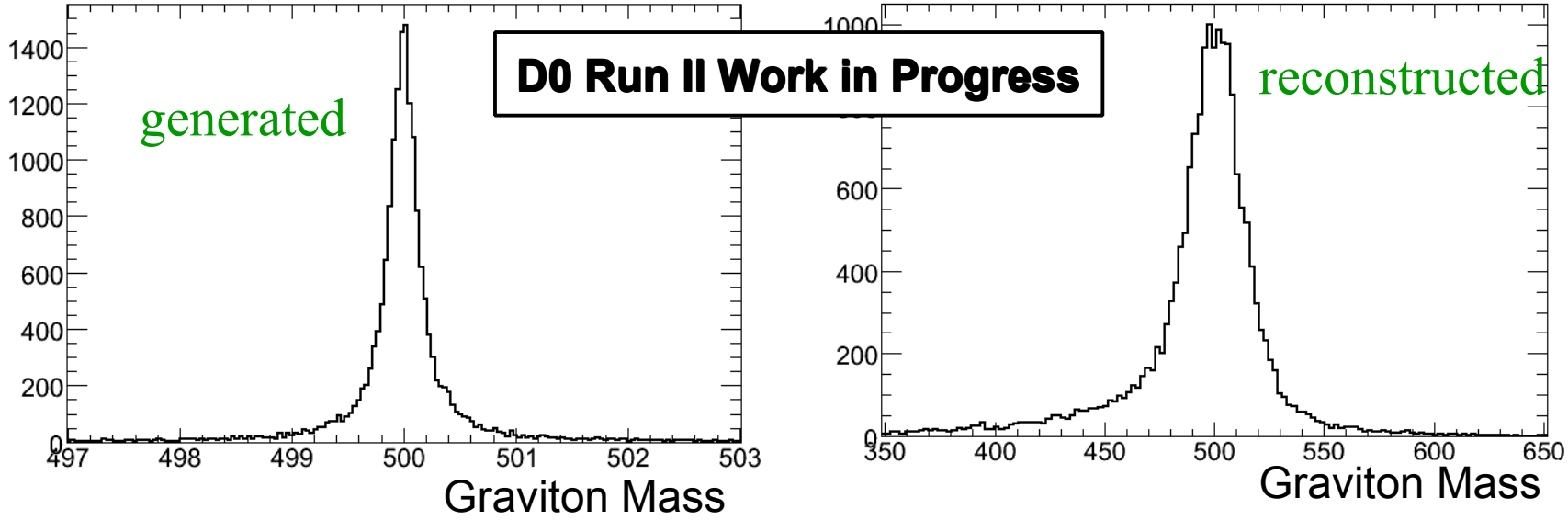

for example, *G->γγ* signal (mass 500GeV with coupling of 0.02)

at generation level, Breit-Wigner fitted width is 300MeV

the mass resolution from reconstruction is 11.5GeV

Graviton Signal (cont'd)

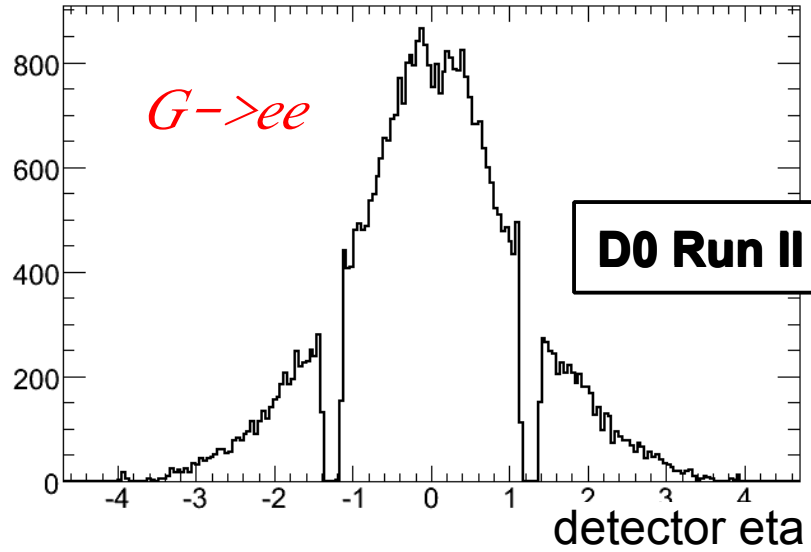

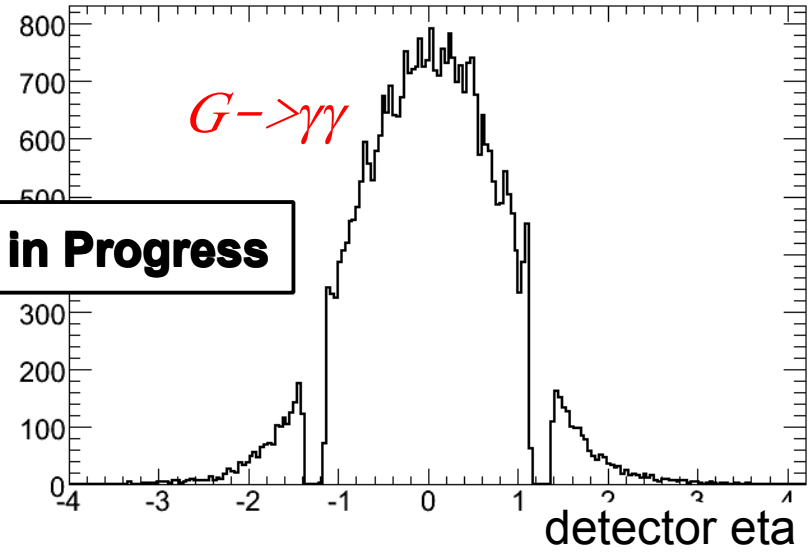

D0 Run II Work in Progress

final state electron detector η distribution in graviton e^+e^- decay (500GeV, 0.02)

photon detector η distribution in 500GeV graviton γγ decay (500GeV, 0.02)

Most of the electrons and photons in graviton decay are produced in the Central Region ($|\eta_{det}| < 1.1$)

Calorimeter Saturation Effect

1. Saturation effects => Nonlinearity in the calorimeter response

2. Using an estimation of saturation energy level for each cell, we estimate this effect on reconstructed energy in graviton MC samples.

Plot: energy in different calorimeter layers of electrons from 1TeV graviton decay with and without saturation effect corrections.

black: without saturation correction
red: with correction

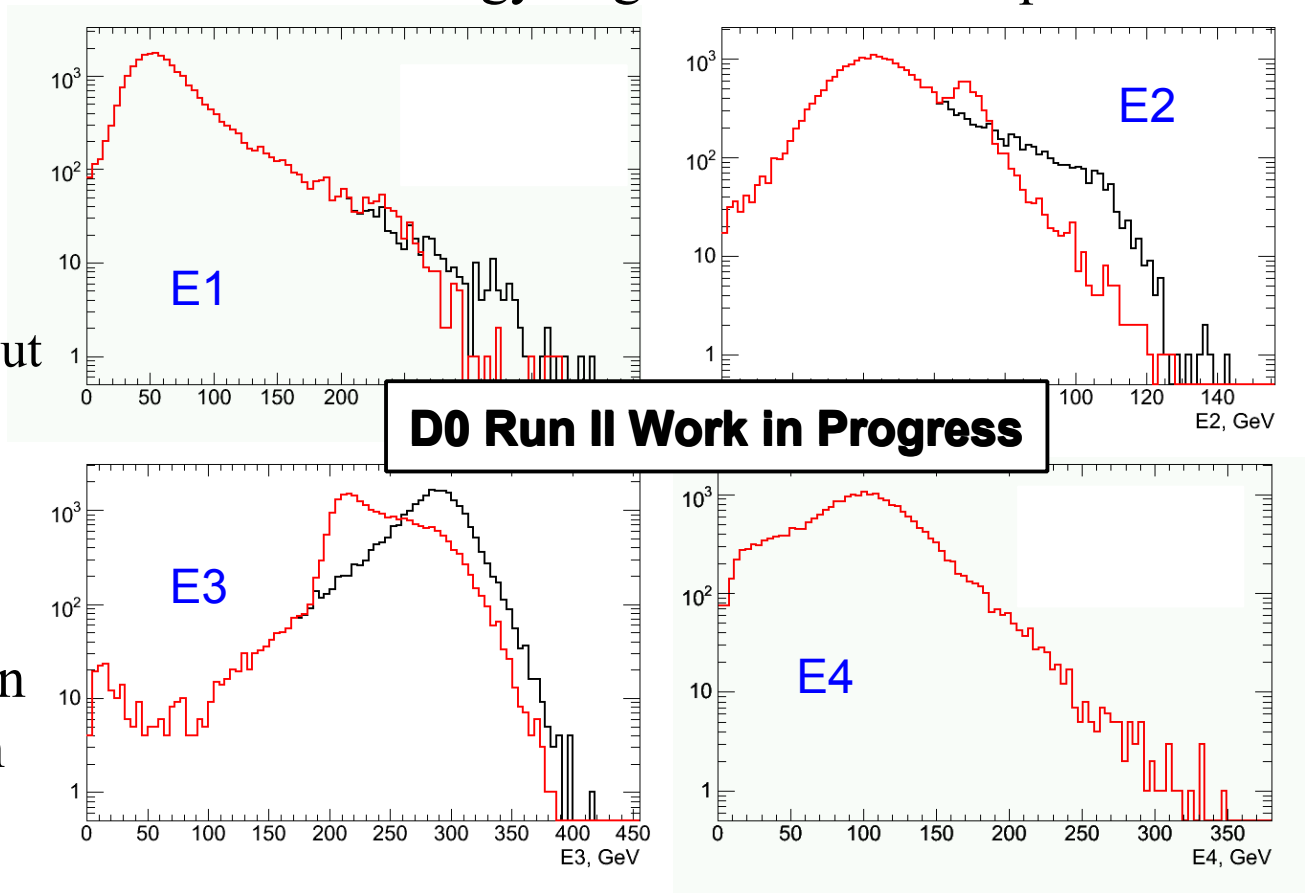

Saturation Effect on Signal Shape

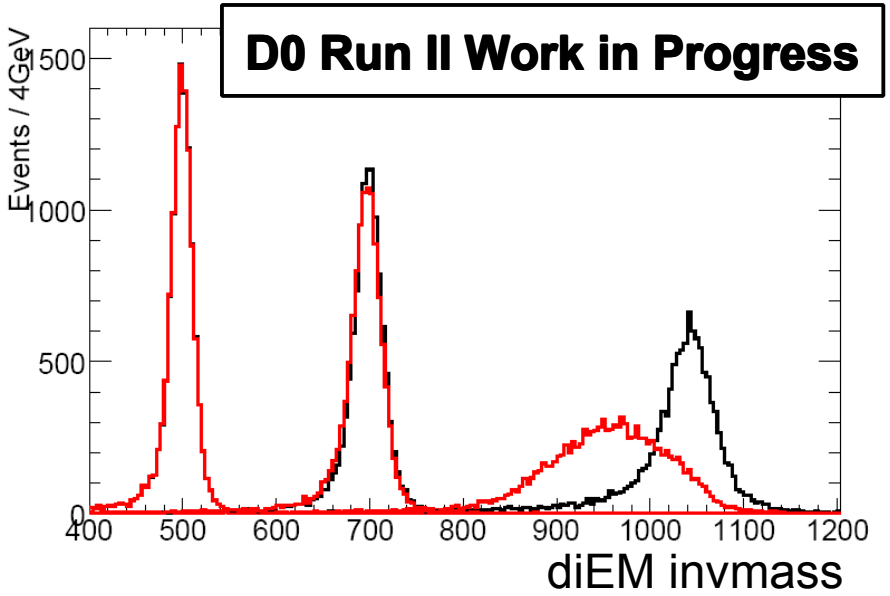

Left: reconstructed di-EM invariant mass distribution of 500GeV, 700GeV and 1050GeV graviton samples (from left to right).

Bottom: Gaussian fitted mean and sigma vs generated graviton mass.

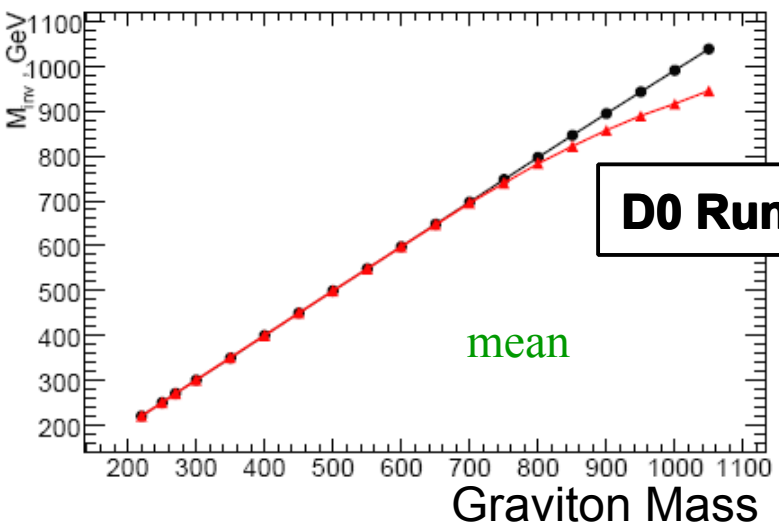

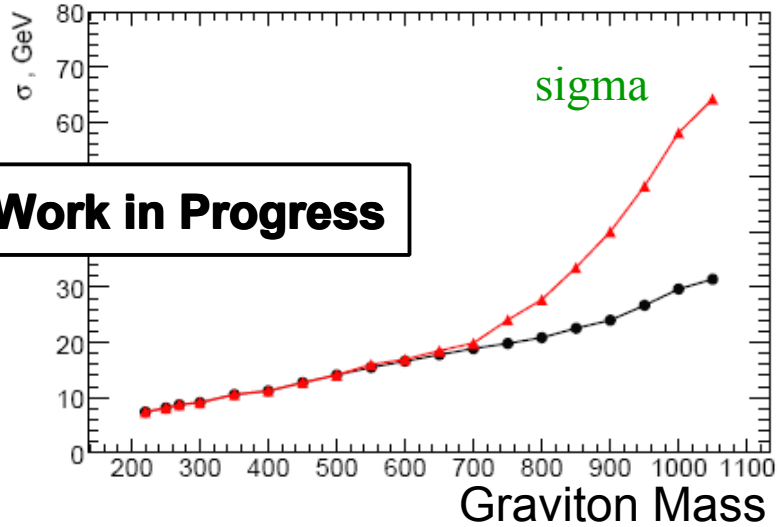

Drell-Yan e^+e^- Background

Drell-Yan ee : PYTHIA

A mass-dependent NNLO/LO k-factor is applied.

5% uncertainty is taken for the k-factor.

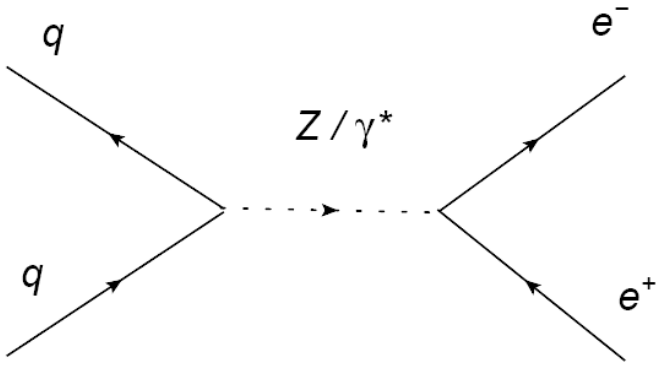

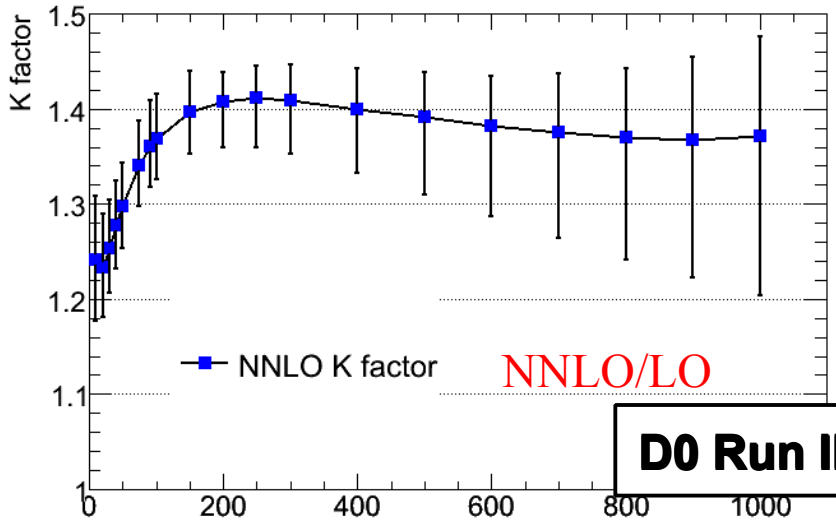

D0 note 4476

Mee

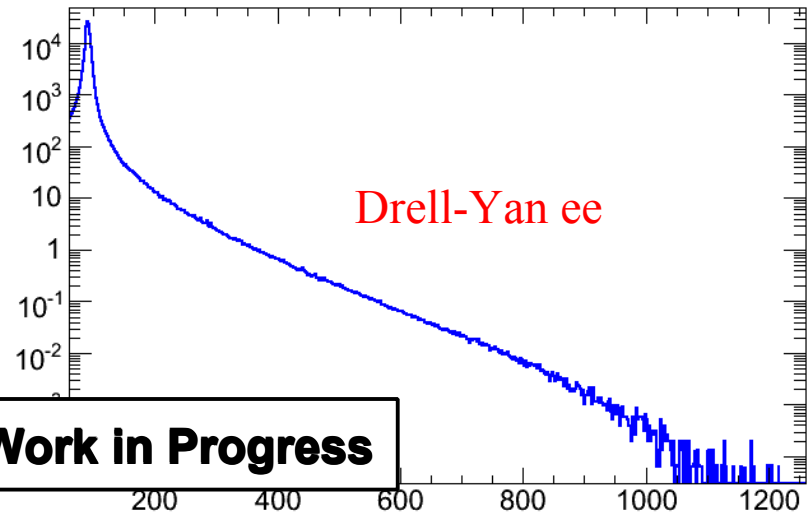

D0 Run II Work in Progress

Mee

QCD γγ Background

QCD γγ : PYTHIA

The PYTHIA spectrum is reweighted to the prediction of full NLO γγ calculation provided by DIPHOX.

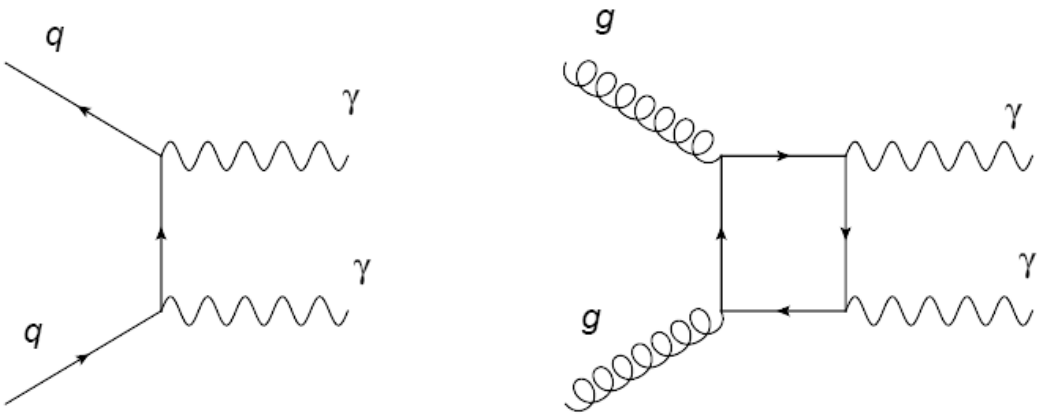

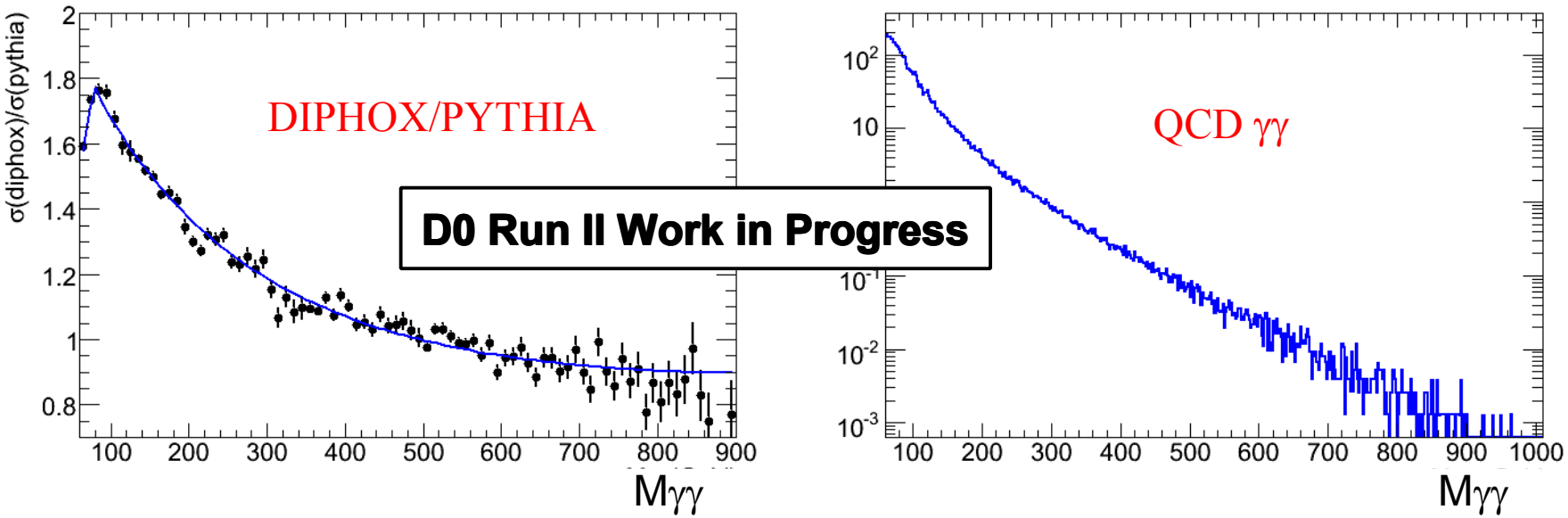

QCD γγ Background (cont'd)

Three arbitrary scales in DIPHOX: renormalization scale μ , initial state factorization scale M and the fragmentation scale M_f.

default: $\mu = M = M_f = m_{\gamma\gamma}$

we tried

1) $\mu = M = M_f = m_{\gamma\gamma}/2$; 2) $\mu = M = M_f = 2m_{\gamma\gamma}$;

3) $\mu = 2m_{\gamma\gamma}$ $M = M_f = m_{\gamma\gamma}/2$; 4) $\mu = m_{\gamma\gamma}/2$ $M = M_f = 2m_{\gamma\gamma}$

variations of total background w.r.t the one from default scale setting

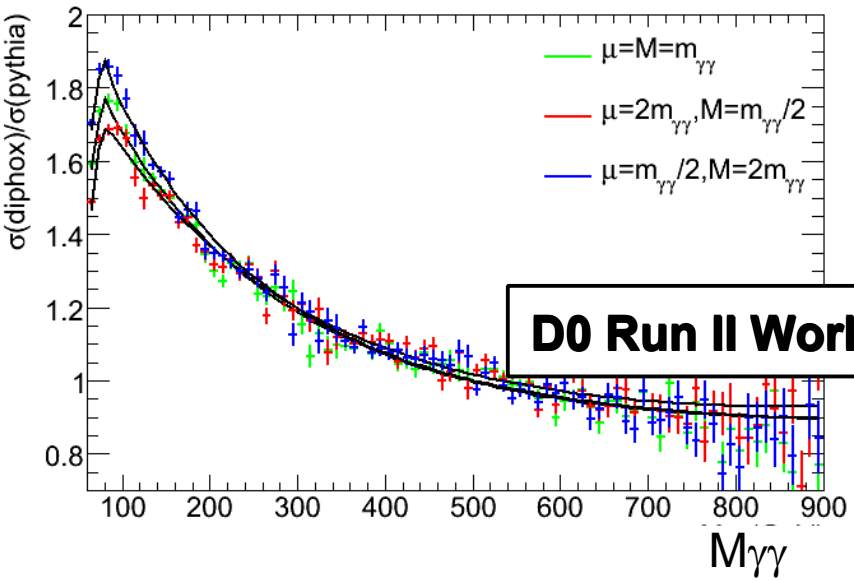

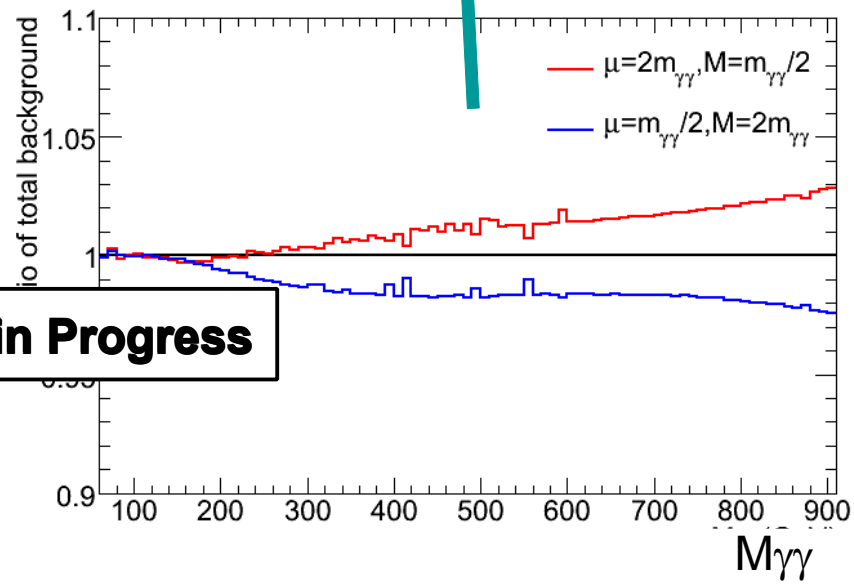

D0 Run II Work in Progress

Instrumental Background

Instrumental Background : electrons or photons faked by jets

- "di-electron" : jet+jet
- "di-photon" : γ+jet and jet+jet
- The shape is estimated from data by reversing calorimeter showershape cut to select a jet-rich sample which is incompatible with EM showers.

Other SM Background : PYTHIA

W+γ, Z−>$\tau\tau$, WZ, WW, ttbar, W+jet

- Their contributions are small.
- W+γ sample is normalized to the measured cross section.
- The others are normalized to the SM NLO prediction.

Primary Vertex

"di-electron" : two high pT tracks,

default primary vertex selection algorithm is efficient at finding correct production vertex.

"di-photon" : without high pT tracks

maxtrk : choose the vertex to which the maximum number of tracks are associated.

cpsmatch : choose the vertex closest to the photon CPS cluster pointing position. In case that neither photon has a CPS cluster matched, "maxtrk" method is used.

Primary Vertex (cont'd)

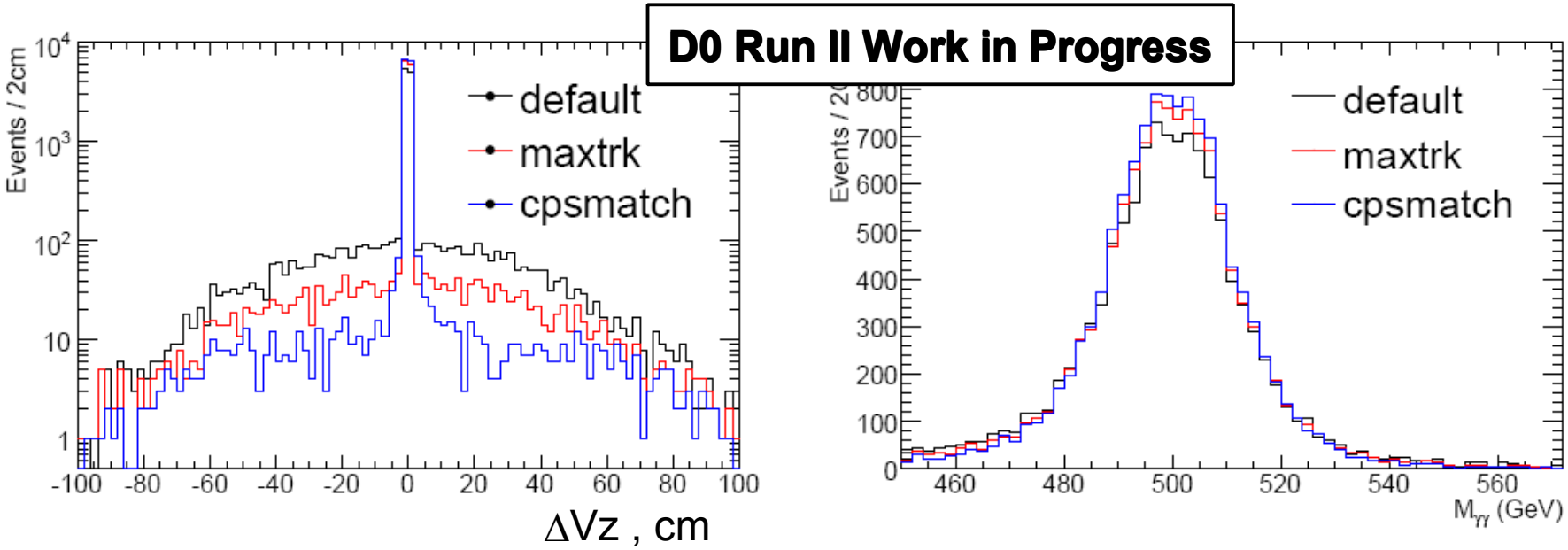

difference between the z-position of the true primary and that selected by the three vertex selection algorithms

diphoton invariant mass distribution, as calculated using the vertex selected by the three algorithms.

For graviton to $\gamma\gamma$ sample (500GeV, 0.02), the graviton mass resolution is improved from 12.3GeV for the "default" to 11.4GeV for the "cpsmatch" algorithm.

Event Selection

1. Data Quality
2. Di-EM Trigger
3. Both EM objects | detector η | < 1.1 and pT > 25GeV
4. Primary vertex $|Z_{vtx}| < 60$ cm
5. Invariant mass > 60GeV
6. Electron ID in "di-electron" channel and Photon ID in "di-photon"

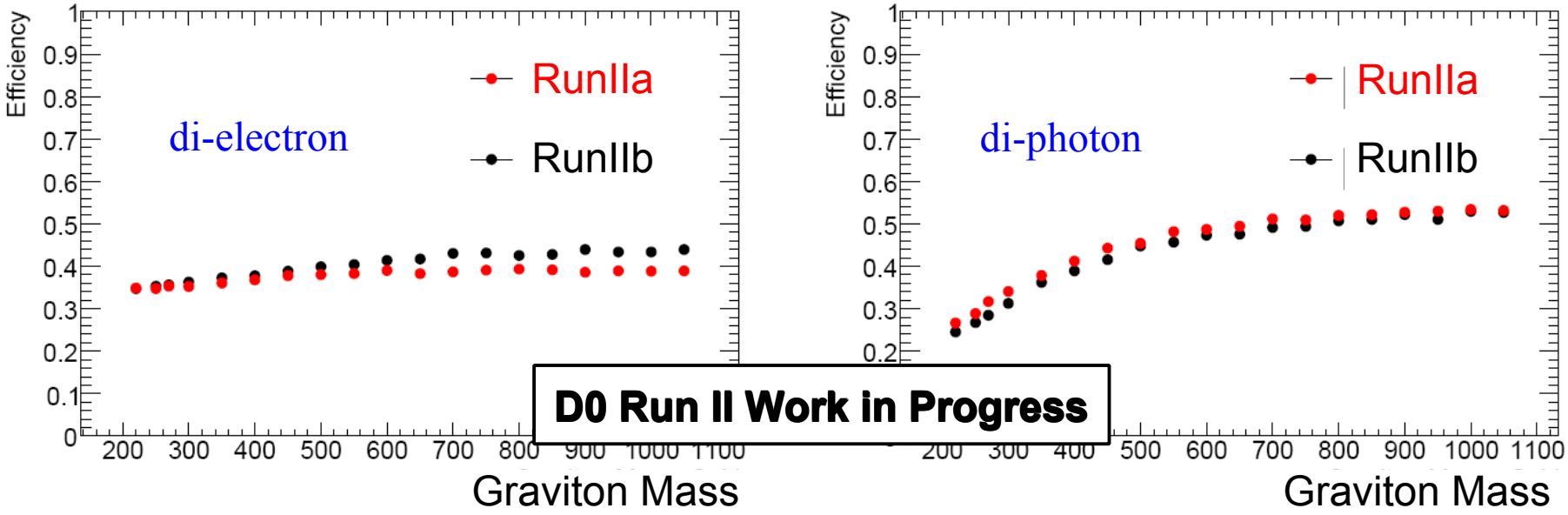

signal selection efficiency of different mass points

Background Normalization

- Fit the data invariant mass h_{data} with h_{bkgnd} in the control region.

$$h_{bkgnd} = f_1 \times h_{DYee} + f_2 \times h_{\gamma\gamma} + (1 - f_1 - f_2) \times h_{jet} + otherSM$$

where $otherSM$ background's normalization is fixed, and h_{DYee} $h_{\gamma\gamma}$ h_{jet} are shape templates. TMinuit gives the f_1 and f_2 values with the smallest Chi2 between h_{data} and h_{bkgnd}

- RunIIa and RunIIb data samples are fitted separately.
- In "di-electron" category, the QCD $\gamma\gamma$ contribution is small and difficult to distinguish from jet background, so its normalization is derived from the fitting results in "di-photon" category.

"Di-Electron" (RunIIa+RunIIb) in Control Region

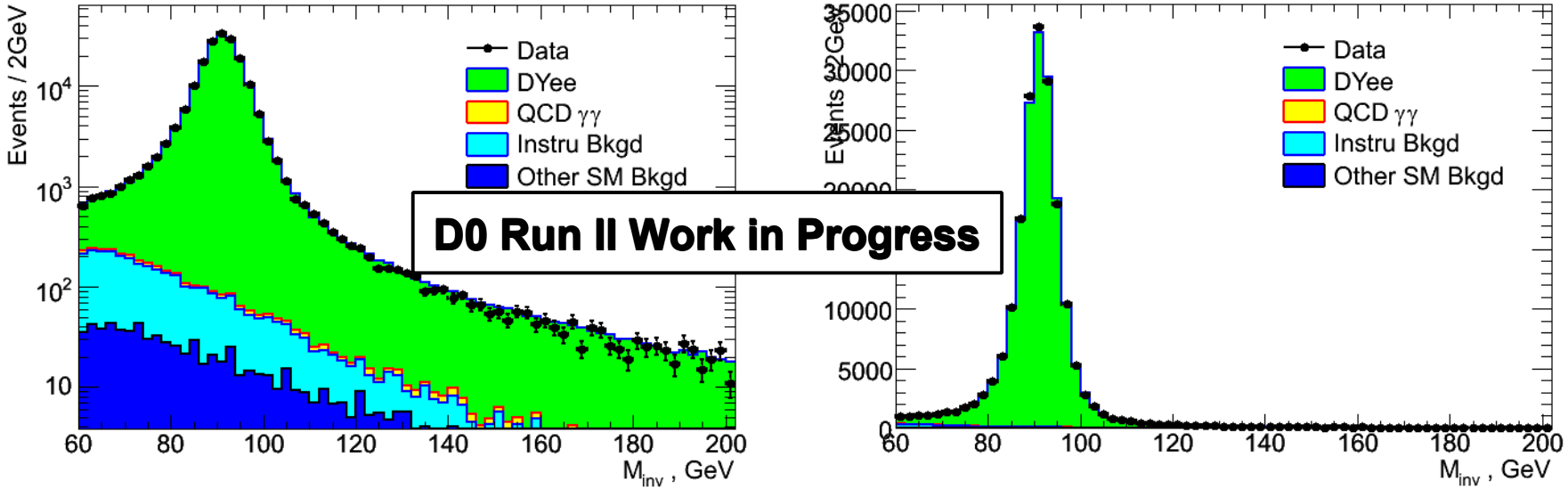

A Chi2 Test between the data and expected background in the control region gives 99/70 (*Chi2/ndof*) in RunIIa sample and 126/70 (*Chi2/ndof*) in RunIIb sample.

Control Region	Data	DY ee	QCD γγ	Instrumental	Others
Num of Evts	186080	182609.0	255.2	2457.8	758.0

"Di-Electron" Over Full Mass Range (RunIIa only)

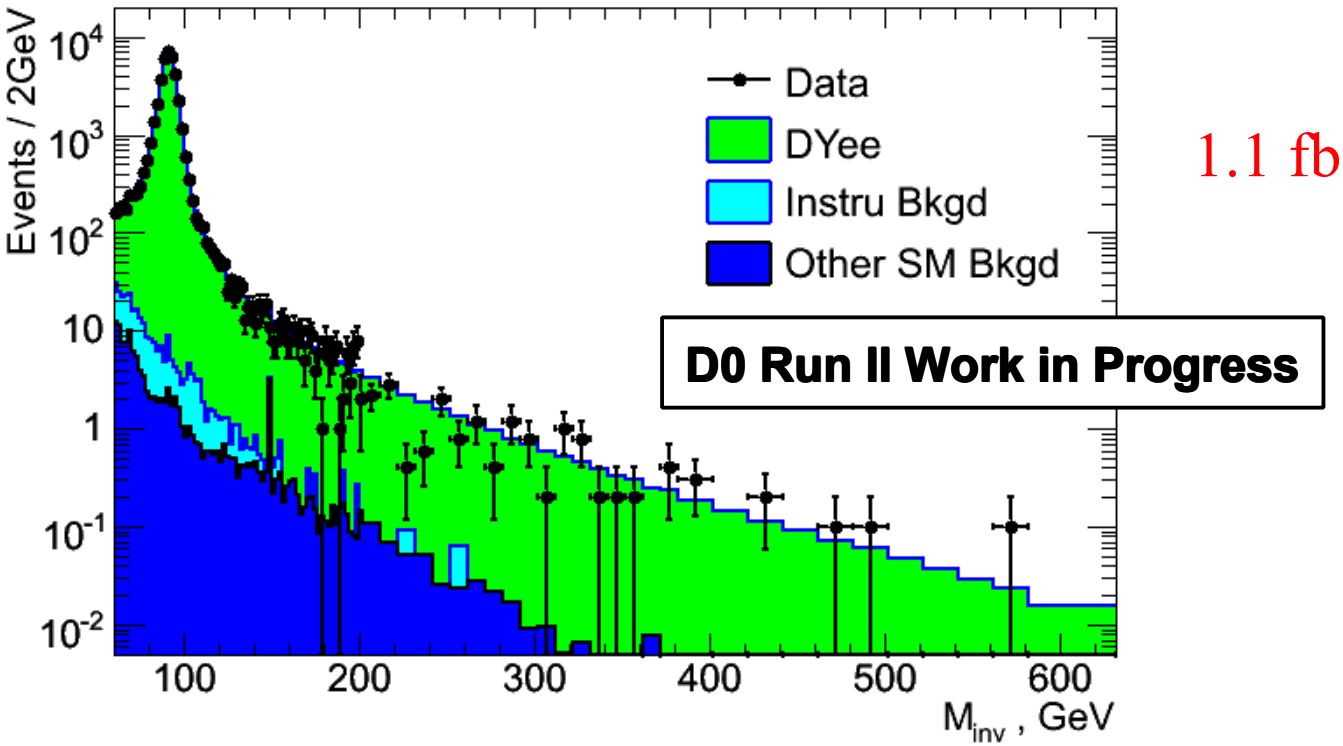

1.1 fb^{-1}

mass window	60-100	100-200	200-300	300-400	400-500	500-600	600-
Data	37599	2366	65	19	4	1	0
Bkgnd	37549.5	2415.5	85.7	17.8	4.9	1.6	0.7

"Di-Photon" (RunIIa+RunIIb) in Control Region

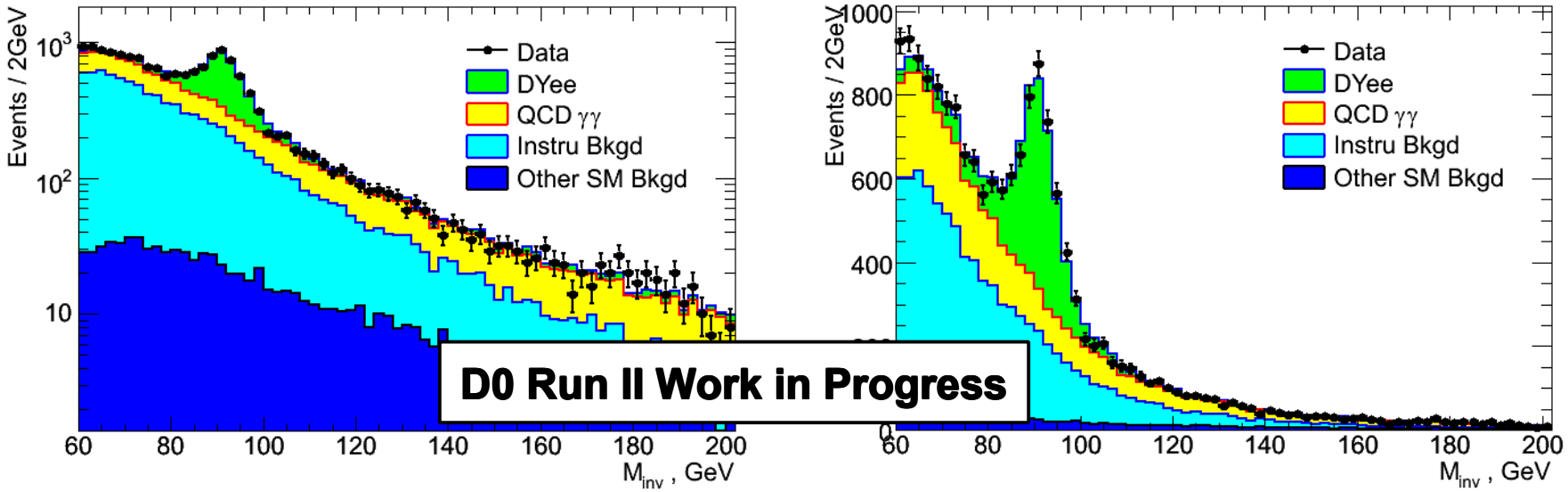

A Chi2 Test between the data and expected background in the control region gives 62/70 (*Chi2/ndof*) in RunIIa sample and 72/70 (*Chi2/ndof*) in RunIIb sample.

Control Region	Data	DY ee	QCD γγ	Instrumental	Others
Num of Evts.	16703	3453.7	4353.0	8030.0	866.3

"Di-Photon" Over Full Mass Range (RunIIa only)

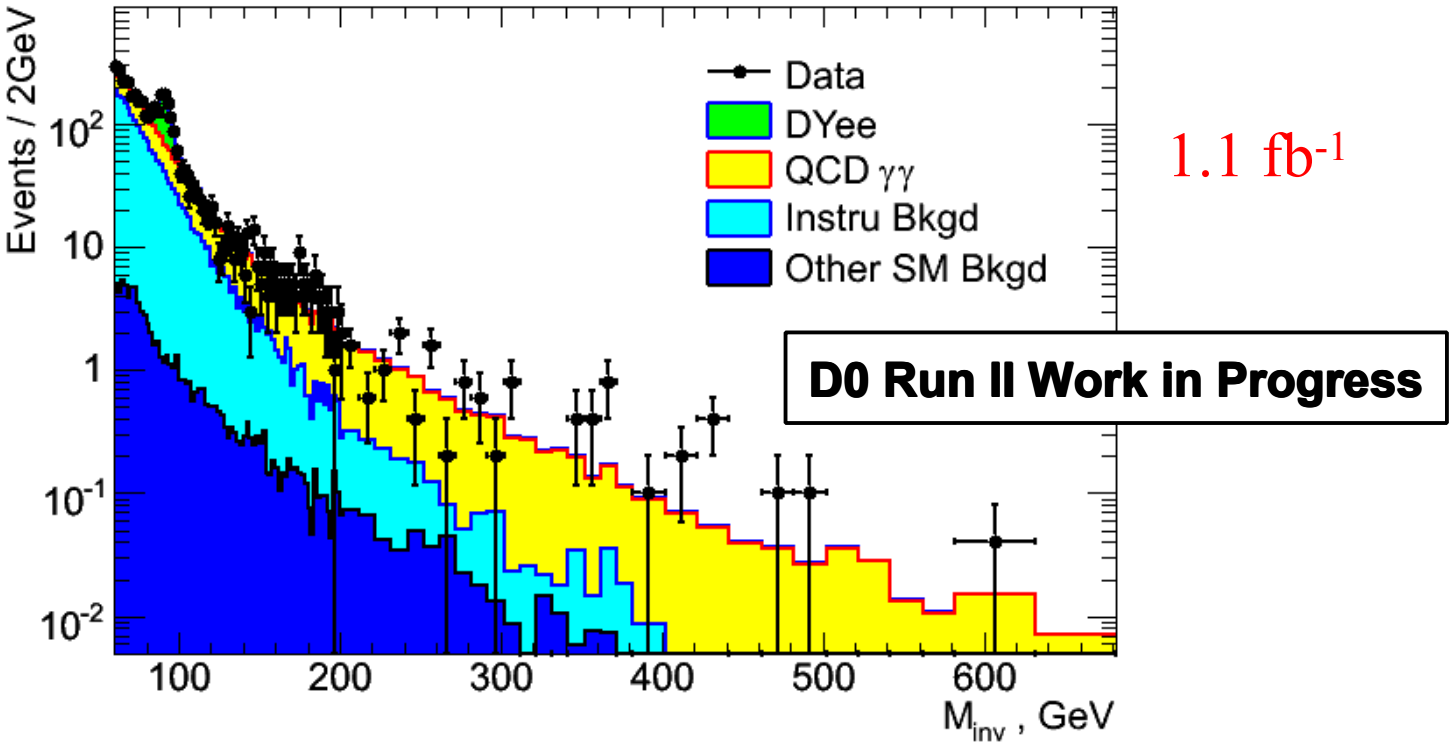

1.1 fb^{-1}

mass window	60-100	100-200	200-300	300-400	400-500	500-600	600-
Data	2949	604	48	13	8	0	1
Bkgnd	2908.5	644.5	51.4	10.0	2.6	1.1	0.6

Systematic Uncertainties

Uncertainties of signal

1. Luminosity: 6.1%
2. Acceptance due to PDF: 0.7% - 6.6% for different mass points
3. Cross section due to PDF: 9.2% - 16.9% for different mass points
4. Energy resolution: mass-dependent
5. EM ID: 3% per EM object

Uncertainties of expected background

1. Drell Yan ee NNLO K-factor: 5.0%
2. QCD $\gamma\gamma$ DIPHOX scales: mass-dependent
3. Background normalization: mass-dependent
4. EM ID: 3% per EM object

Uncertainties from energy resolution, DIPHOX scales, background normalization are mass dependent. The others are taken as constant scales.

Energy Resolution Uncertainty

- For the EM calorimeter, the electron or photon energy resolution can be modeled with three parameters

$$\frac{\sigma_{EM}(E)}{E} = C_{EM} \oplus \frac{S_{EM}}{\sqrt{E}} \oplus \frac{N_{EM}}{E}$$

where C_{EM} is the constant term, N_{EM} is the noise term, and S_{EM} is the sampling term.

- For high energy EM particles, the influence of the constant term is dominant.The value of the constant term is measured as $2.06 \pm 0.12\%$, implying a relative uncertainty of ~6%
- Two Gaussian functions with larger (oversmearing) and smaller (undersmearing) widths are produced for graviton signals, which give weights to each event to simulate these effects on the signal reconstruction.

Background Normalization Uncertainties

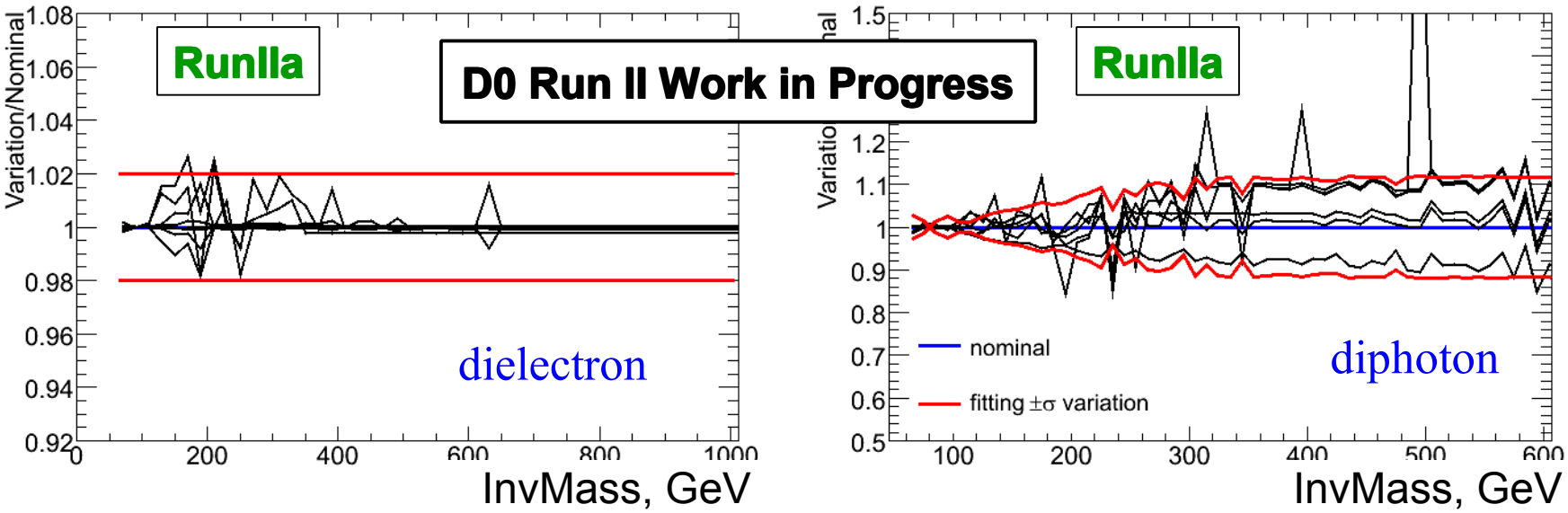

By varying the instrumental background estimation, we estimate the uncertainty of total background.

Plot: Variations of total background w.r.t the nominal one (**black** curves) and uncertainty lines (**red**) in RunIIa

Limit Calculation (RunIIa only)

- In the absence of a signal of a heavy narrow resonance, an upper limit on the cross section times branching ratio on graviton to ee decay is set.
- 19 signal mass points from 220GeV to 1050GeV are tested with a modified-frequentist method.

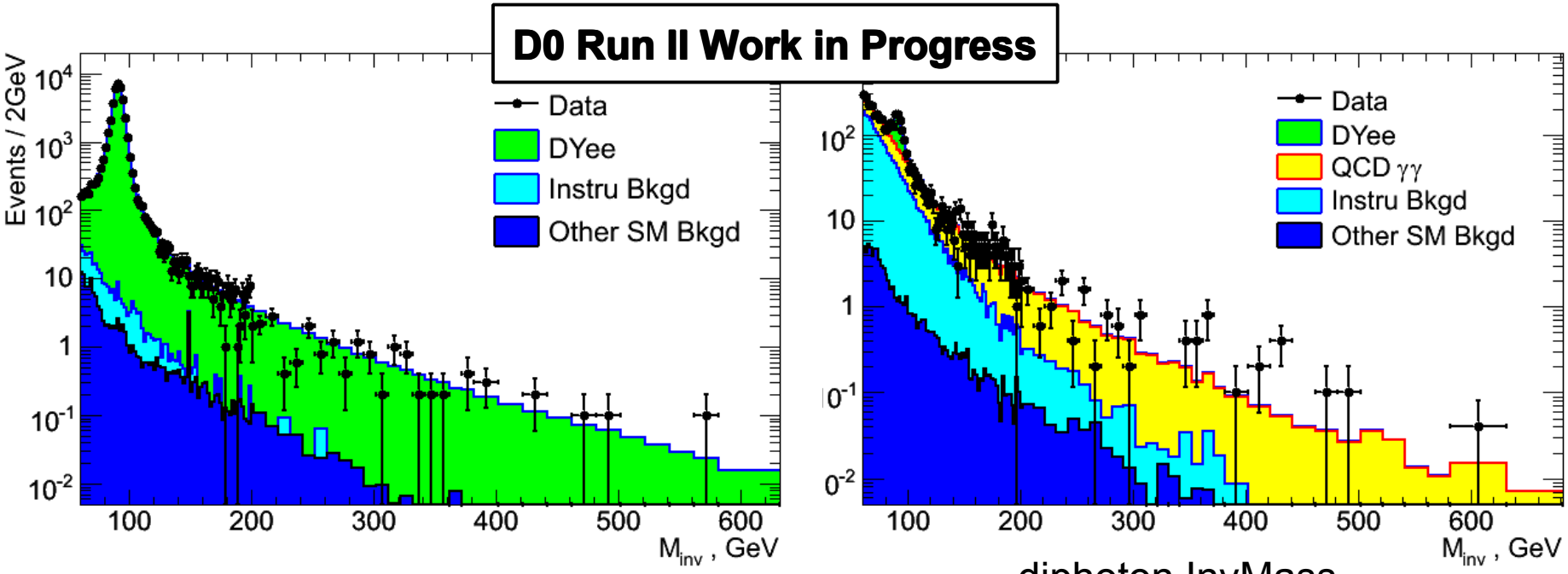

dielectron InvMass

diphoton InvMass

95% CL Exclusion Limits (RunIIa only)

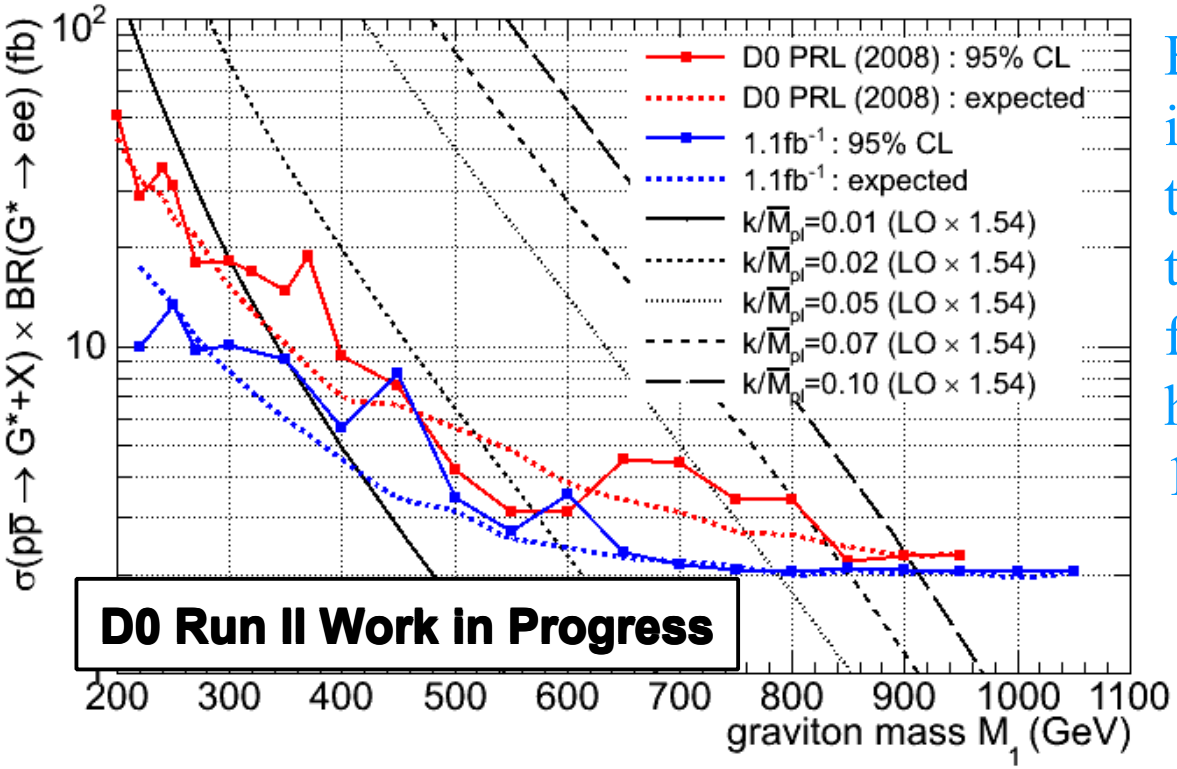

By splitting di-EM channel into ee and γγ channels and tuning the selection ID etc, the improvement obtained from the previous search has a factor of typically 1.5-2.

95% CL exclusion limits on the cross section times $e+e^-$ branching ratio, compared with previous search at DØ, based on RunIIa sample, 1.1fb^{-1}.

95% CL Exclusion Limits (RunIIa only) (cont'd)

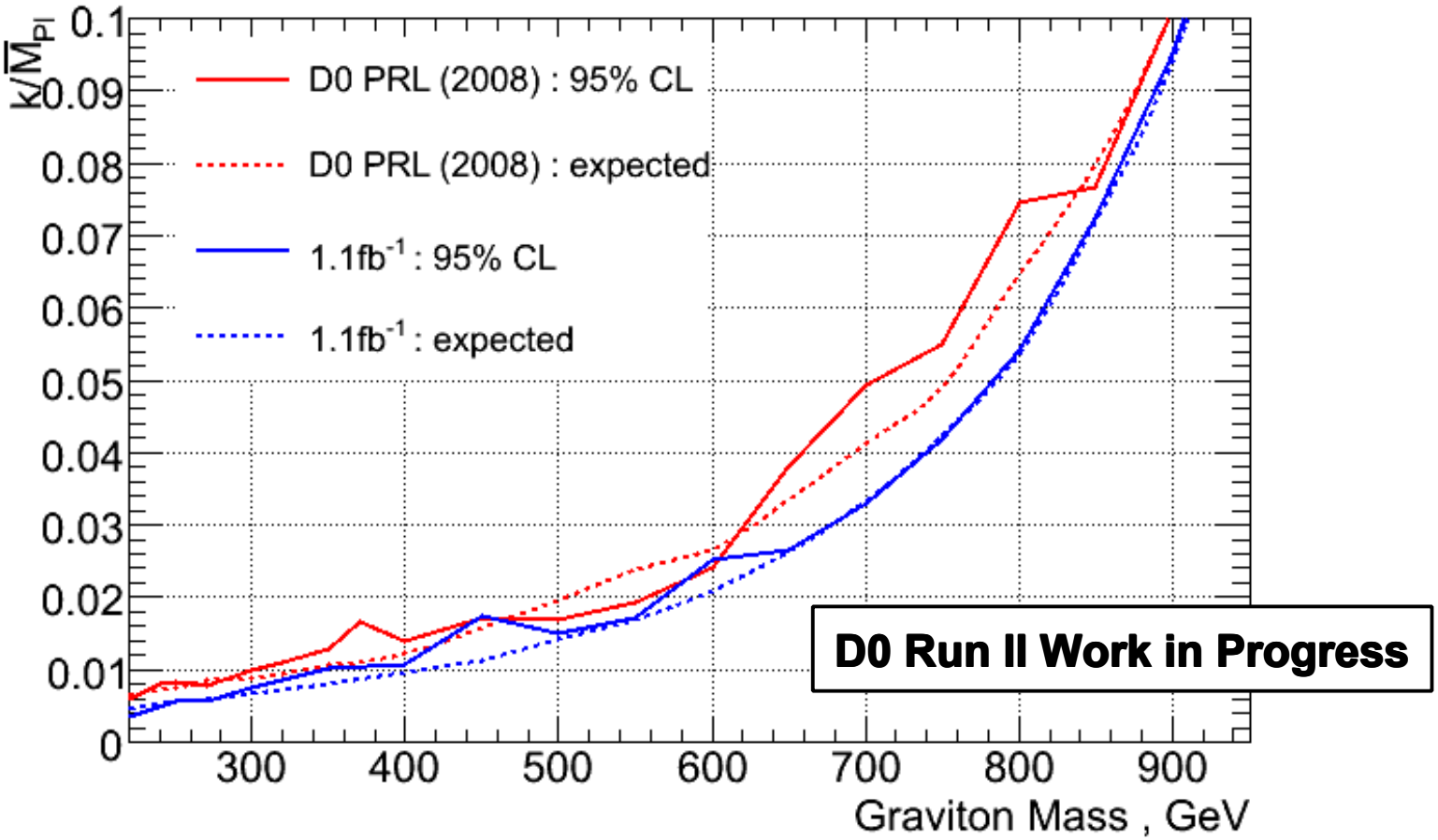

Convert the limits on the cross section times branching ratio into the limits on the RS graviton coupling constant.

Results

- For RunIIa, no significant excess is seen in the data above the expected background level. 95% CL exclusion limits are set.
- Compared to the previous DØ published limits using the same RunIIa dataset, an improvement on the sensitivity by a factor of 1.5-2 is achieved.
- The results with the full dataset are currently undergoing DØ internal review and will be available soon.

Outlook

- DØ is taking data again.
- ~12fb^{-1} delivered by the end of 2011 is expected.
- The S/sqrt(S+B) of graviton search will by improved by a factor of ~1.5 from current 5.4fb^{-1} integrated luminosity.

- Now the LHC is being commissioned; first collisions at 900GeV were recently observed, with operations at 7TeV anticipated during 2010.
- From Tevatron 1.96TeV ppbar to LHC 14TeV pp
- Graviton (500GeV, 0.01 for instance) to ee cross section times branching ratio (LO) increases from 1.1 fb to 187.4 fb, by a factor of ~110. For Z to ee (M>60GeV) (LO) it increases from 179.4 pb to 2015 pb, by a factor of ~11.

Discovery Potential at ATLAS

- With center of mass 14TeV and 1fb^{-1} integrated luminosity at LHC
- Randall Sundrum graviton with mass 900GeV and coupling 0.01 would be at 5σ discovery level if existing.
- In case a signal is observed, could use angular distribution for spin discrimination.

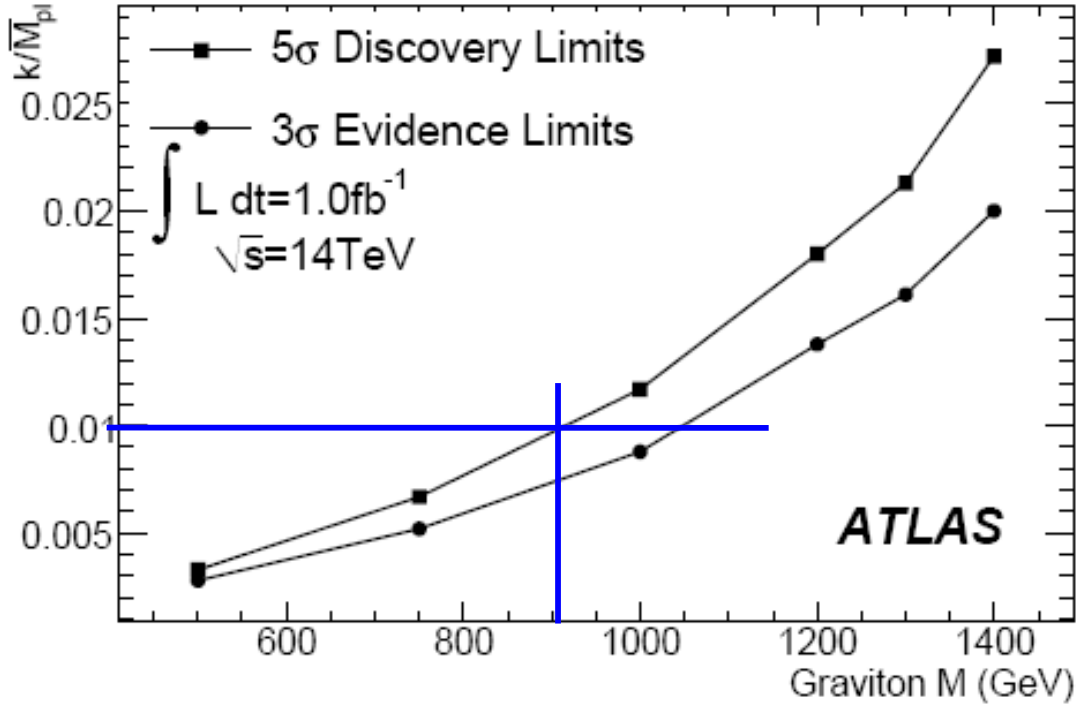

Signal and Background Angular Distriubiton at ATLAS

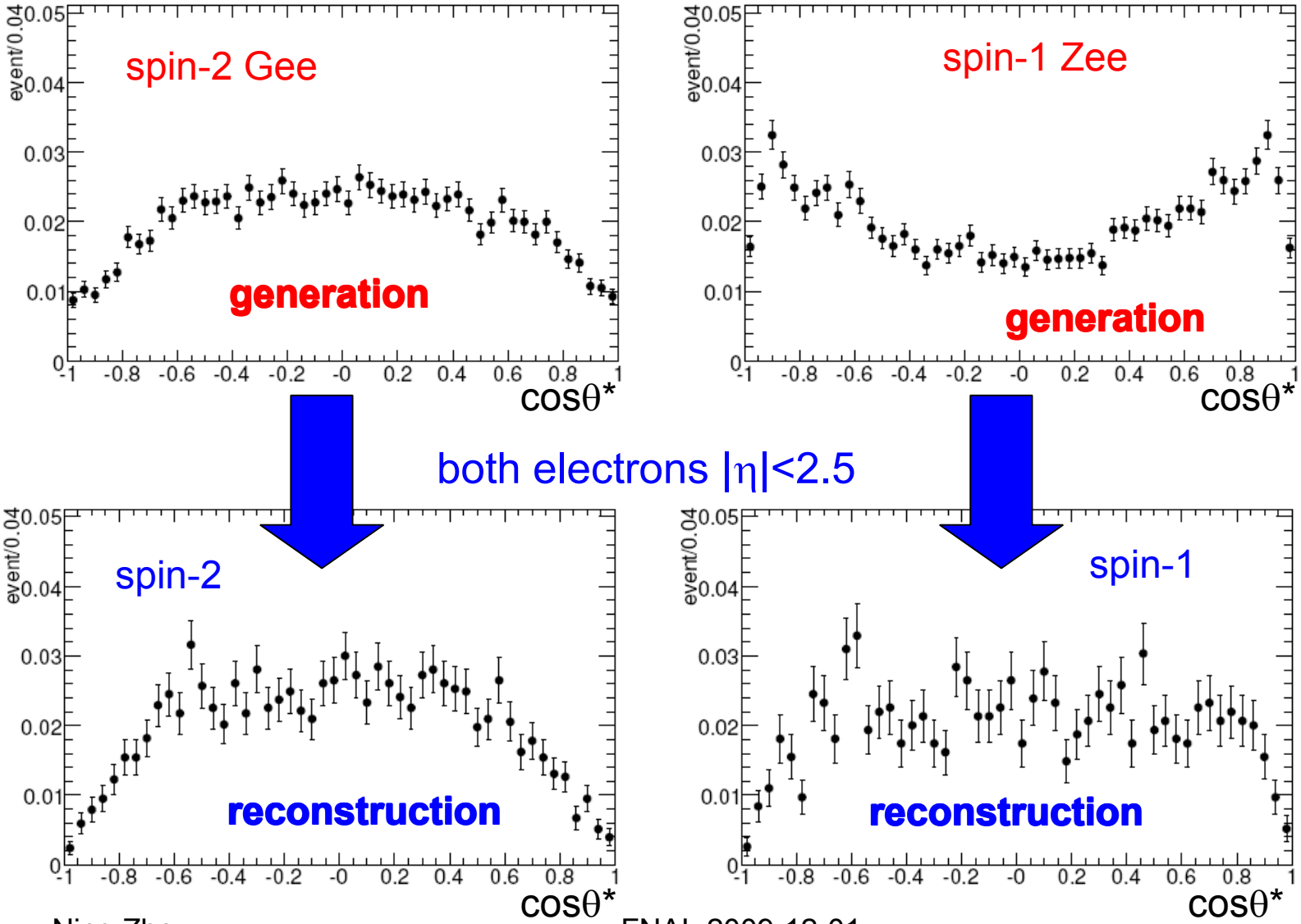

Forward EM clusters at ATLAS

- Electrons in the forward region |η|>2.5, would help to improve the spin discrimination.
- Forward EM cluster identification.

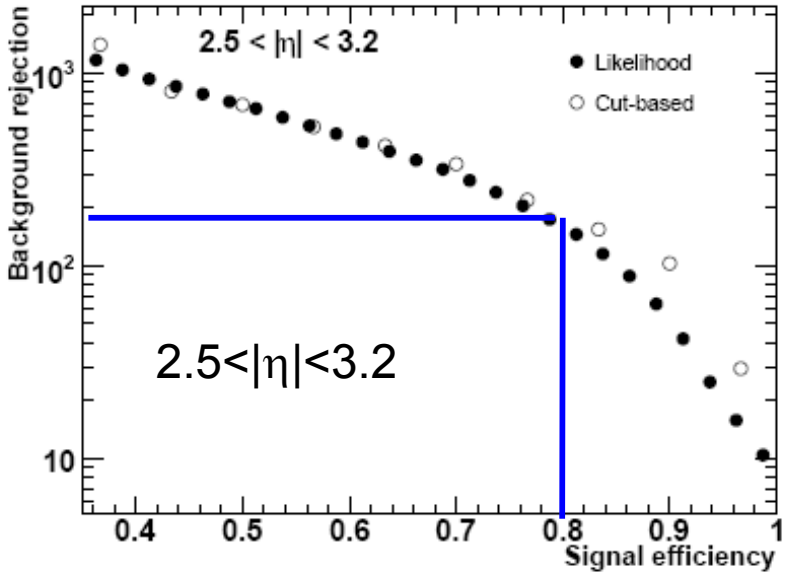

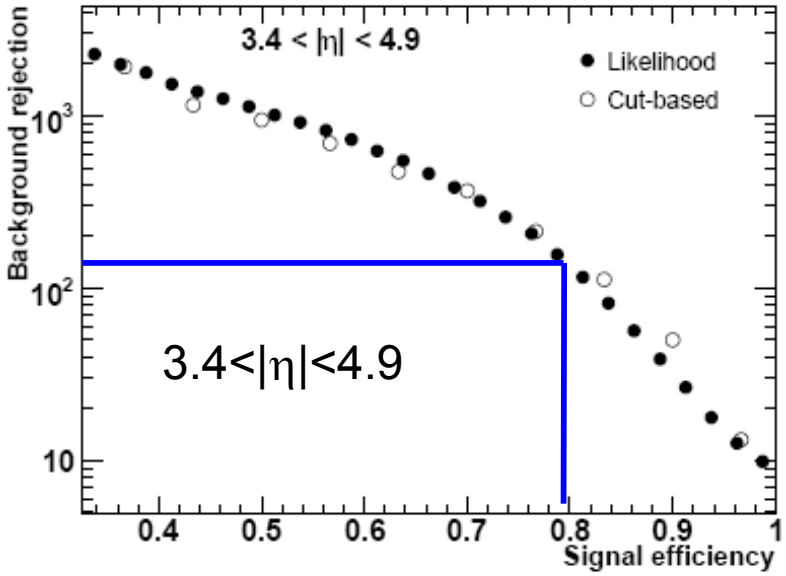

jet rejection rate vs signal efficiency

- For signal efficiency of 80%, ~ 1% jet fake rate is expected.

Angular Distribution with Forward Electrons at ATLAS

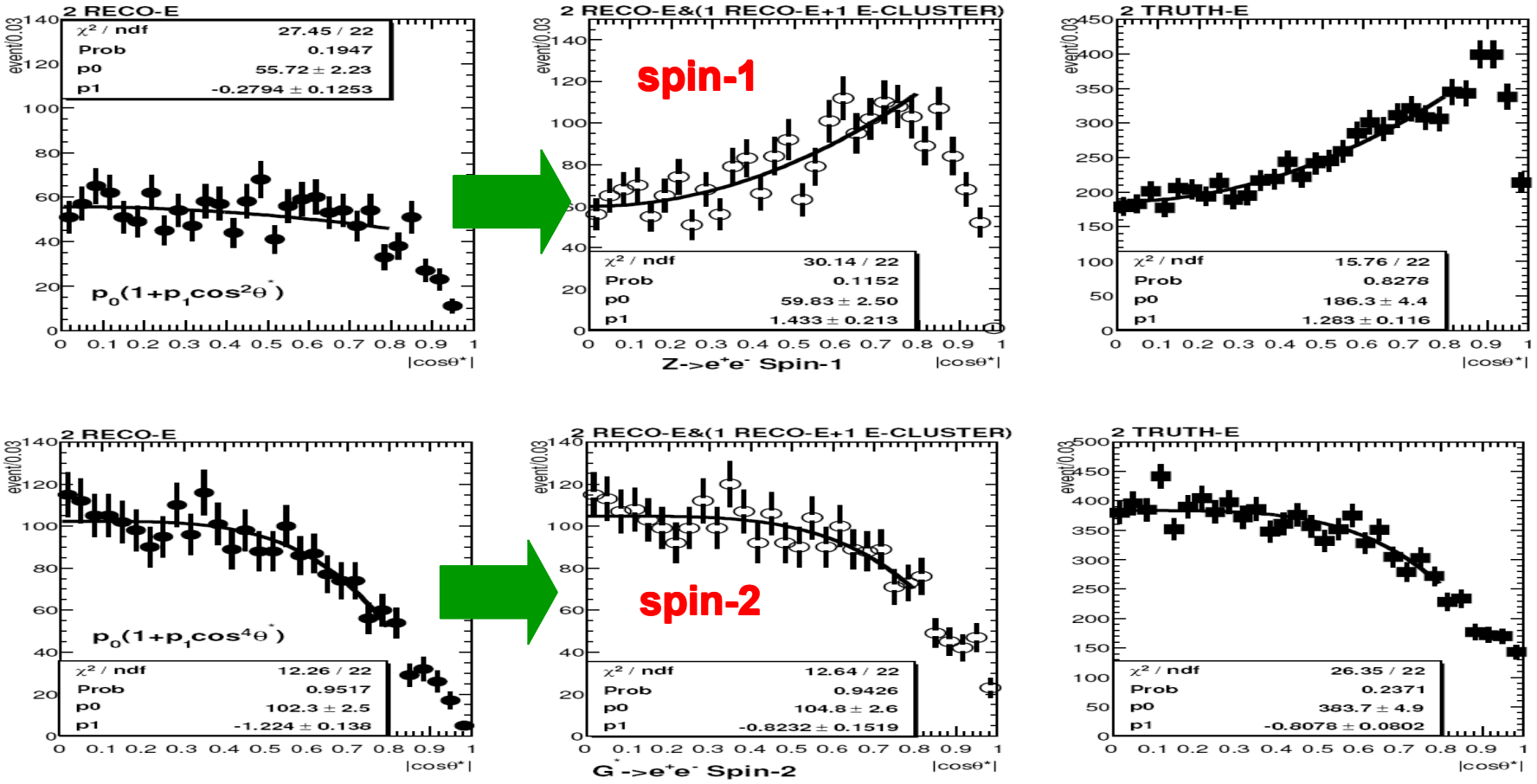

both $|\eta|<2.5$

both $|\eta|<2.5$ + one $|\eta|<2.5$ and one forward electron

at generation level

Summary

- $5.4 fb^{-1}$ of DØ data is used for this analysis.
- For RS graviton signals, we search for a resonance in the di-EM invariant mass spectrum.
- To improve the signal sensitivity, di-EM events are split into two non-overlapping categories "di-electron" and "di-photon", based on the tracking information. EM ID is tuned for "di-electron" and "di-photon" categories separately.
- Improvement from DØ previous published result is achieved.
- Full dataset result is undergoing internal review.

Thanks!

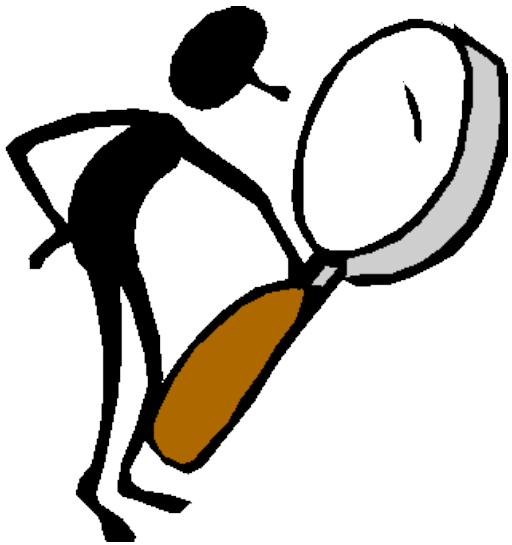

BACKUPS

Limit Calculation (cont'd)

- Invariant mass spectrum of "di-electron" and "di-photon" categories.
- A modified-frequentist method

$$\Gamma = -2\ln(Q) = 2\sum_{i=1}^{Nchannels}\sum_{j=1}^{Nbins}(s_{ij} - d_{ij}\ln(1 + s_{ij}/b_{ij}))$$

where s and b are the signal and expected background, d is the data

- 19 signal mass points from 220GeV to 1050GeV are tested.

Signal PDF Uncertainty

- PDF reweight procedure: central pdf set CTEQ6M and 40 sets of error pdfs
- For each event, a weight is calculated for each pdf set relative to the leading order pdf set CTEQ6L. A quadratical summation of all the positive (negative) differences gives the positive (negative) uncertainty. The larger one of the positive and negative uncertainties is taken.

For graviton (500GeV, 0.02)

Acceptance uncertainty : 1.1% in ee channel, 5.4% in $\gamma\gamma$ channel

Cross section uncertainty : 11% in both ee and $\gamma\gamma$ channel

Angular Distribution

upper plot: fraction of quark-antiquark contribution in graviton production. (from Pythia CTEQ6L1). Above 220GeV, quark-antiquark dominates the process.

lower plot: normalized angular distributions of different processes.

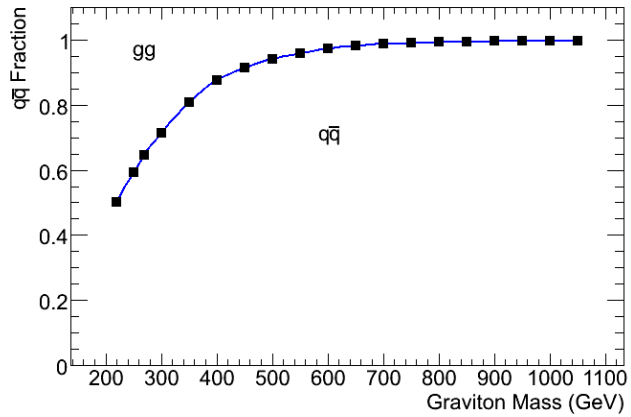

The angular distribution could be used for graviton search together with invmass.

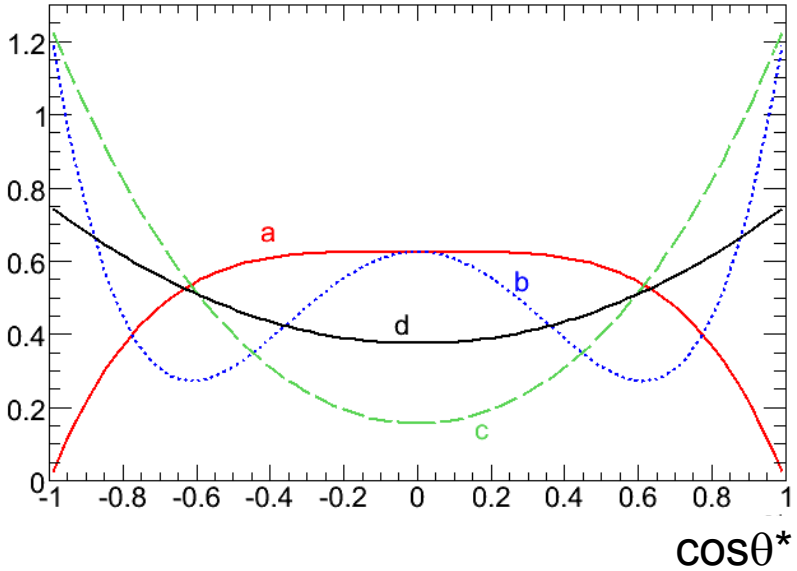

Process	Distribution	Plot
$gg \to G \to f\bar{f}$	$\sin^2\theta^*(2-\beta^2\sin^2\theta^*)$	a
$q\bar{q} \to G \to f\bar{f}$	$1+\cos^2\theta^*-4\beta^2\sin^2\theta^*\cos^2\theta^*$	b
$gg \to G \to \gamma\gamma$	$1+6\cos^2\theta^*+\cos^4\theta^*$	c
$q\bar{q} \to G \to \gamma\gamma$	$1-\cos^4\theta^*$	a
$q\bar{q} \to \gamma^*/Z^0/Z' \to f\bar{f}$	$1+\cos^2\theta^*$	d

Angular Distribution - CCCC

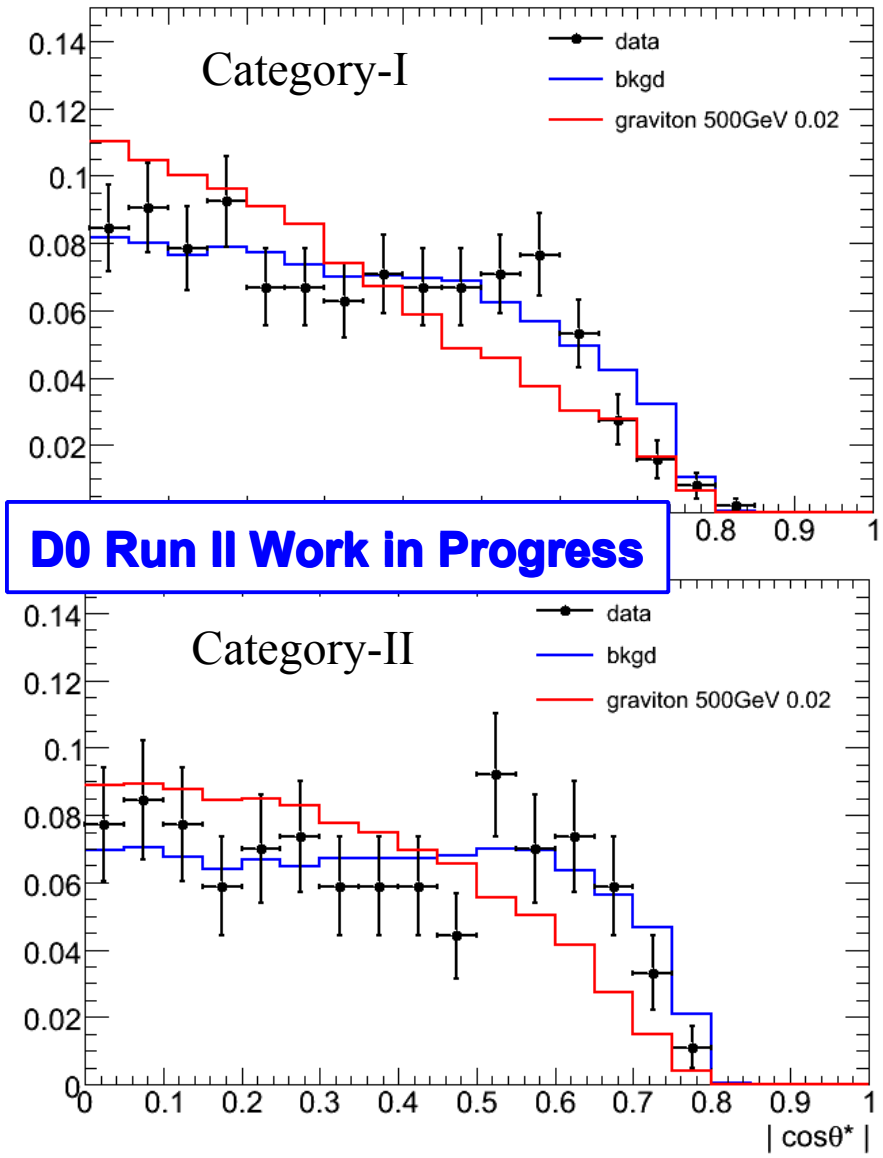

The plots show the normalized angular distributions for M_{inv}>200GeV with CC-CC events (Both $|\eta_{detector}|<1.1$)

However, as seen in the plots, CC-CC cuts off most of high $|\cos\theta^*|$ region where the discrimination power is located.

test with the angular distribution:
inputs to limit calculation package
2-dimensional histograms
M_{inv} vs $|\cos\theta^*|$

Exclusion Limits with Angular Info

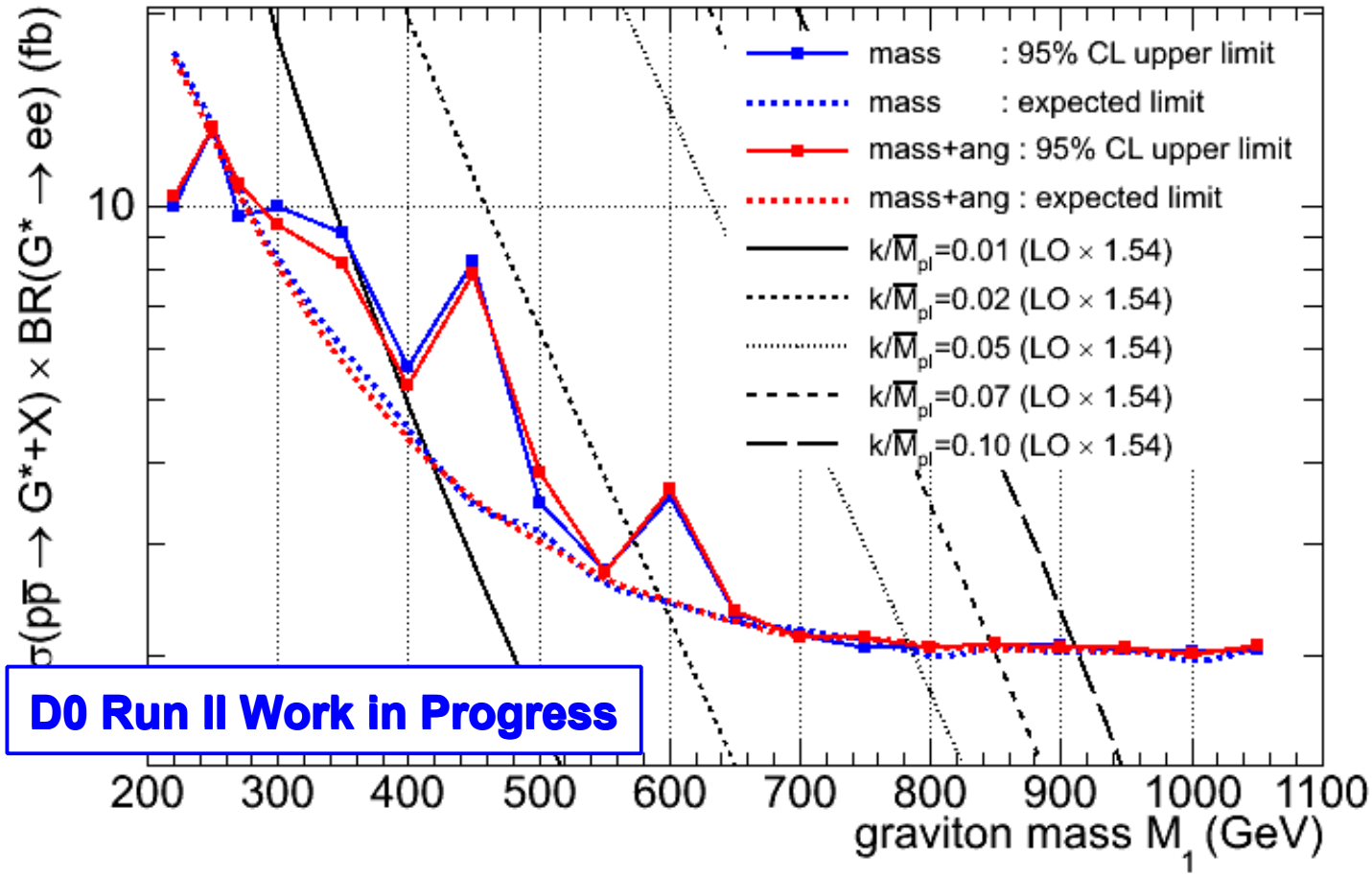

Exclusion limits from combination of invmass and angular distributions. There is no large improvement achieved, as expected.

EM ID at DØ

1. Loose electron ID and photon ID are used in Category-I and Category-II respectively.

2. The selection efficiency is ~ 90% and jet rejection rate after preselection is ~30-50.

3. Besides a cut on the track matching probability, different multivariate variables are tuned for electrons and photons separately.

4. The electron ID efficiency and scale factor (Data/MC) is provided by EMID group.

5. I took part in the photon ID efficiency and scale factor measurement in the EMID group.

Photon ID

1. The photon ID is split into calorimeter-only selection and track-based selection.
2. For the calorimeter-only selection, the scale factor is estimated from electron sample with large statsitics.
3. Electron sample is selected from the data via Tag and Probe method, fake electron contamination is removed by template-fitting method.

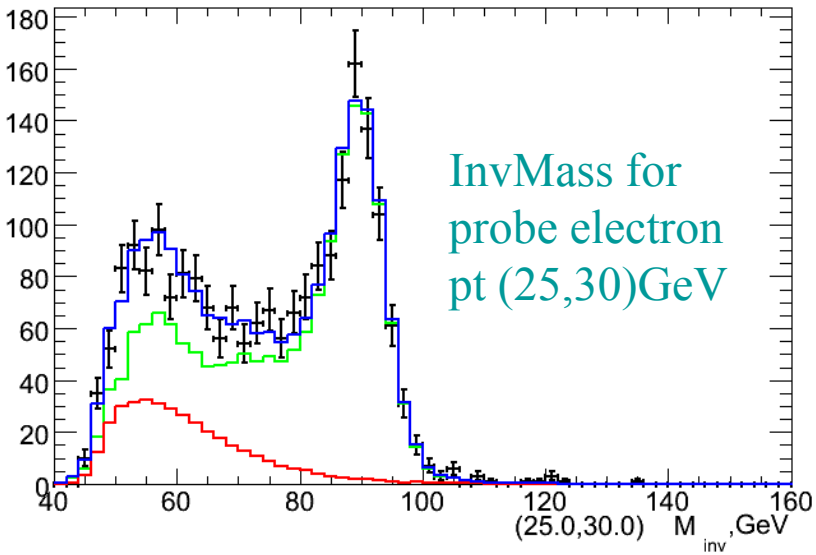

with DYee invmass template (**green**) from MC and jet template (**red**) from data, we fit the full range invmass of tag and probe electrons. **blue**: combination of DYee and jet templates with proper normalization derived from the fitting.

Photon ID (cont'd)

4. For track-based selection, the scale factor is measured from photon samples by selecting Z-> ll+γ events.

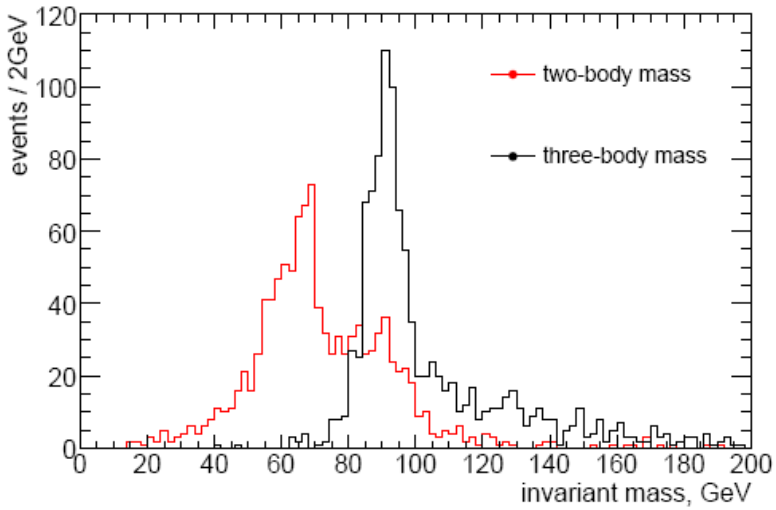

Distributions of μμ two-body mass (**red**) and μμγ three-body mass (**black**).

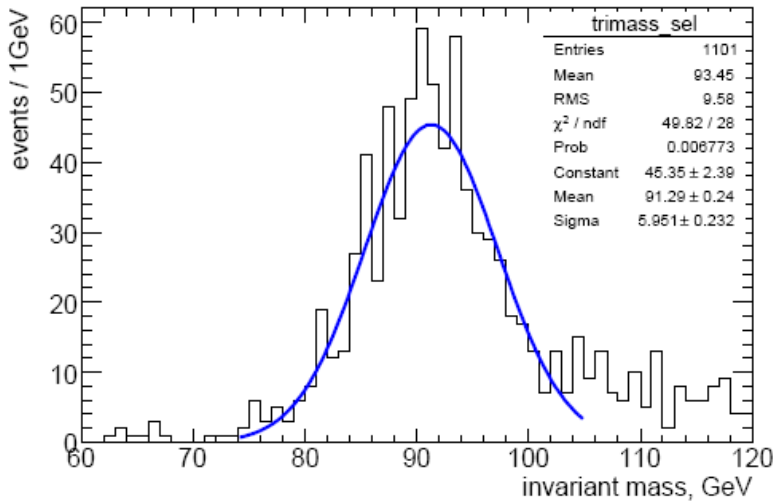

Detailed look on the three-body invariant mass under Z peak

Track and Preshower

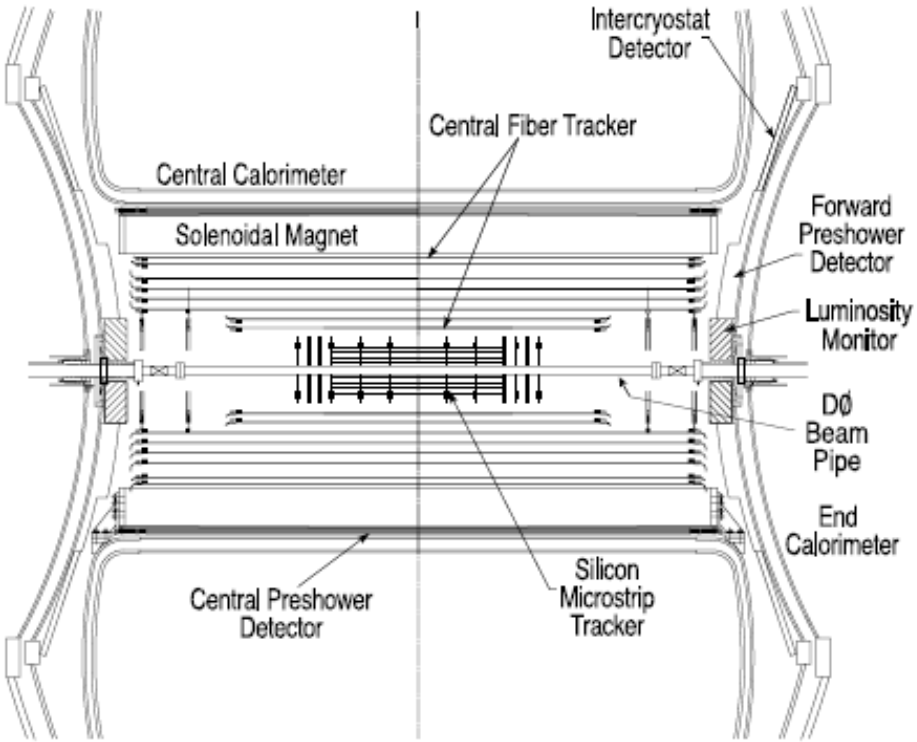

SMT: silicon mictrostrip tracker. Accurate tracking and vertexing for $|\eta_{det}| < 2.5$

CFT: central fiber tracker, providing tracking up to $|\eta_{det}| \sim 1.7$

Solenoidal Magnet: 2T

Preshower detectors: CPS, FPS electron-photon separation and improving spatial matching between central tracks and calorimeter energy clusters.

DØ central tracking system. The SMT centered around the beam pipe, is surrounded by the CFT. Also shown are parts of the calorimeter system and the luminosity monitors.

Calorimeter

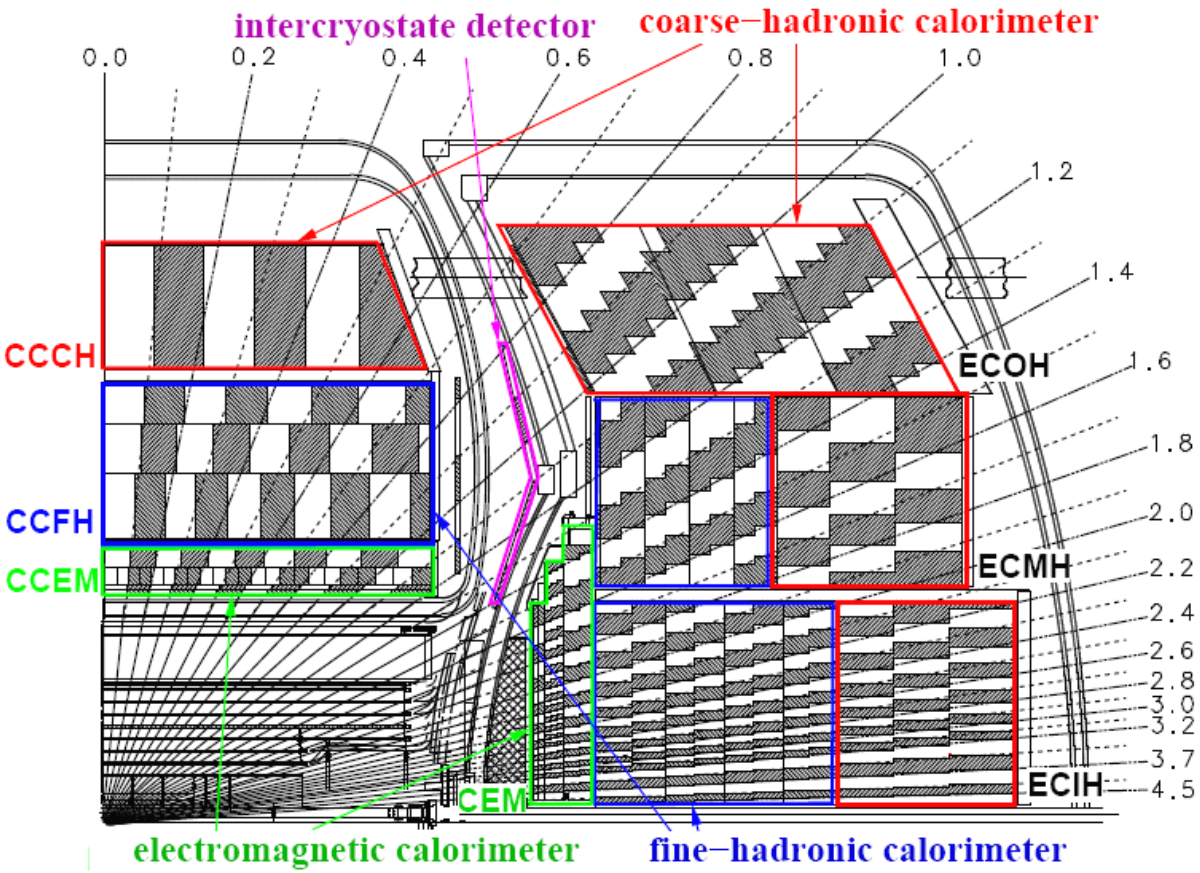

side-view of one quarter of the DØ calorimeter system. The shading shows the segmentation into psedu-projective towers.

1. absorb and measure the energy of all particles, except for muons and neutrinos.
separate hadronic jets from electrons and photons.
2. the central calorimeter (CC, $|\eta_{det}|<1.1$) and two endcap calorimeters (EC, upto $|\eta_{det}|\sim4.0$).
3. electromagnetic (EM) calorimeter, fine hadronic (FH) and coarse hadronic (CH) calorimeters.
4. EM ~ $20X_0$, $0.8\lambda_A$
total ~ $7\lambda_A$

Muon, Luminosity and Trigger

Muon System three-layered muon system

1. proportional drift tubes, $|\eta|<1.0$
2. mini drift tubes in addition to scintillators, $|\eta|<2.0$
3. toroid, between the first and the two last layers, 1.6-1.8T
4. no coverage in the downward direction $4.25<\phi_{det}<5.15$

Luminosity Monitor

1. Two arrays of 24 plastic scintillator counters at $z=\pm 140$cm $2.7<|\eta_{det}|<4.4$.
2. determine the instantaneous luminosity at D0 interaction point.

$$L = \frac{1}{\sigma(p\bar{p}, effective)} \cdot \frac{dN}{dt}(p\bar{p})$$

σ: inelastic ppbar collision cross section

3. fast measurement of the interaction vertex z coordinate, vertex multiplicity, beam halo rates

Trigger 1.7MHz - L1 - 2kHz - L2 - 1kHz - L3 - 50Hz

Electrons and Photons Reconstruction

Calorimeter: EM, FH, CH

1. a dR=0.2 cone algorithm using calorimeter towers based on the four EM and the first hadronic calorimeter layers.
2. narrow lateral shape of the calorimeter shower
3. shower shape of electrons is nearly identical with that of photons
4. $$E^{measured} = \alpha \cdot \sum_{i=1}^{5} \beta_i A_i + \delta$$

where A_i is the calorimeter singalin each of the five layers, β_i is the relative response correction of the five layers with β_3=1.0, α is the overal calibration factor, δ is an energy offset correction which can arise from energy loss in material before the calorimeter, noise, energy from additional ppbar interaction and from signal being lost due to zero suppression.

5. energy resolution $$\frac{\sigma_{EM}(E)}{E} = C_{EM} \oplus \frac{S_{EM}}{\sqrt{E}} \oplus \frac{N_{EM}}{E} \qquad C_{EM} = 2.06 \pm 0.12\%$$

Electron and Photon Reconstruction (cont'd)

Tracking System: SMT, CFT

1. Vertex reconstruction,
2. Track reconstruction

   Probablity of a spatial track matching,

   "Hits on the road" which utilizes the hit information from the CFT and SMT detectors to estimate the probability fo EM object to be either a photon or an electron.

Preshower detector : CPS, FPS

1. Preshower cluster shower shape
2. With good spatial resolution, CPS provides "pointing" information.

   CPS pointing spatial resolution is measured as 3.6cm.

   Photon production vertex identification from CPS pointing

Instrumental Background

"di-electron" : jet+jet => reverse calorimeter shower shape cut on both EM objects

"di-photon" : γ+jet and jet+jet => reverse cut on either of the two EM objects.

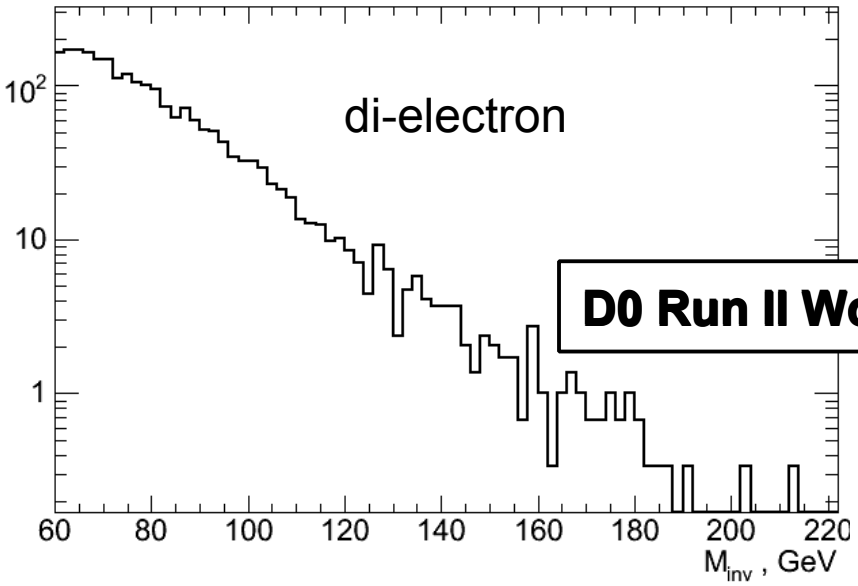

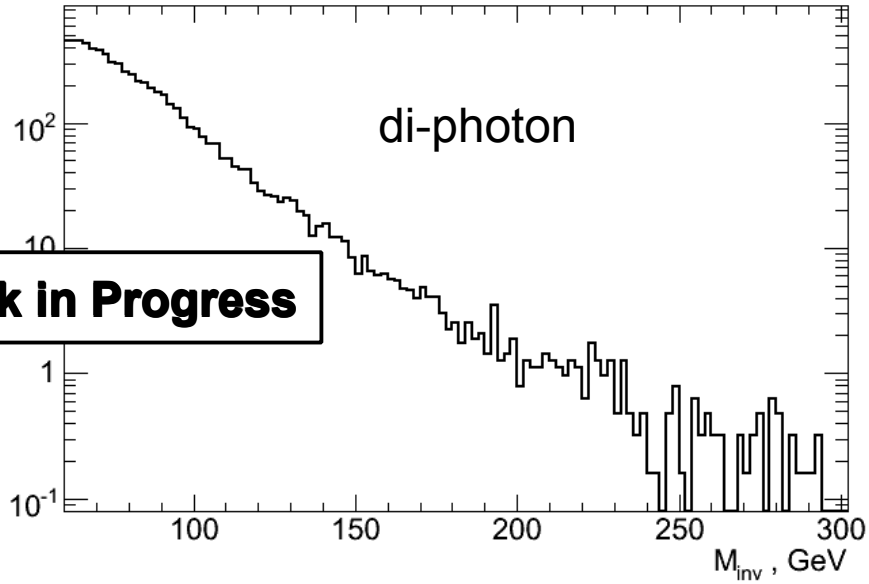

D0 Run II Work in Progress

Bkgnd Normalization Uncertainties in Category I

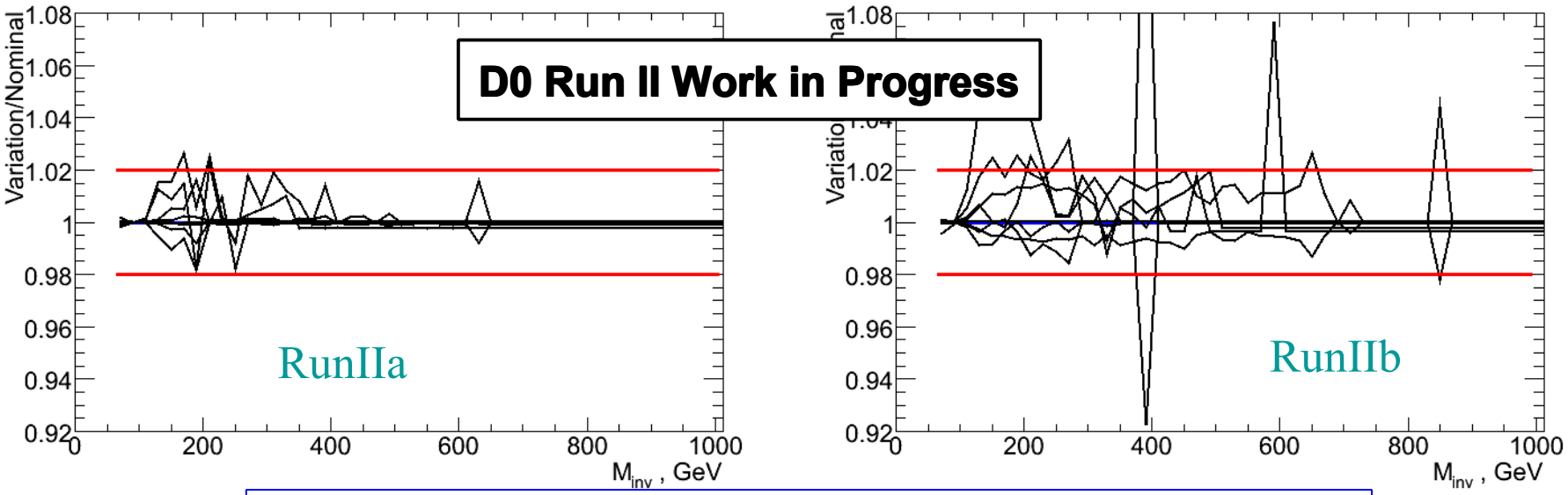

variation of total background w.r.t to the nominal one

1. TMinuit gives the fitting uncertainty of DY ee contribution ~0.2%
2. By varying the instru background estimation and $\gamma\gamma$, W+jet normalizations, we estimate the uncertainty of total background, the black curves on the plots.
3. 2% is taken as a conservative value.

Bkgnd Normalization Uncertainties in Category II

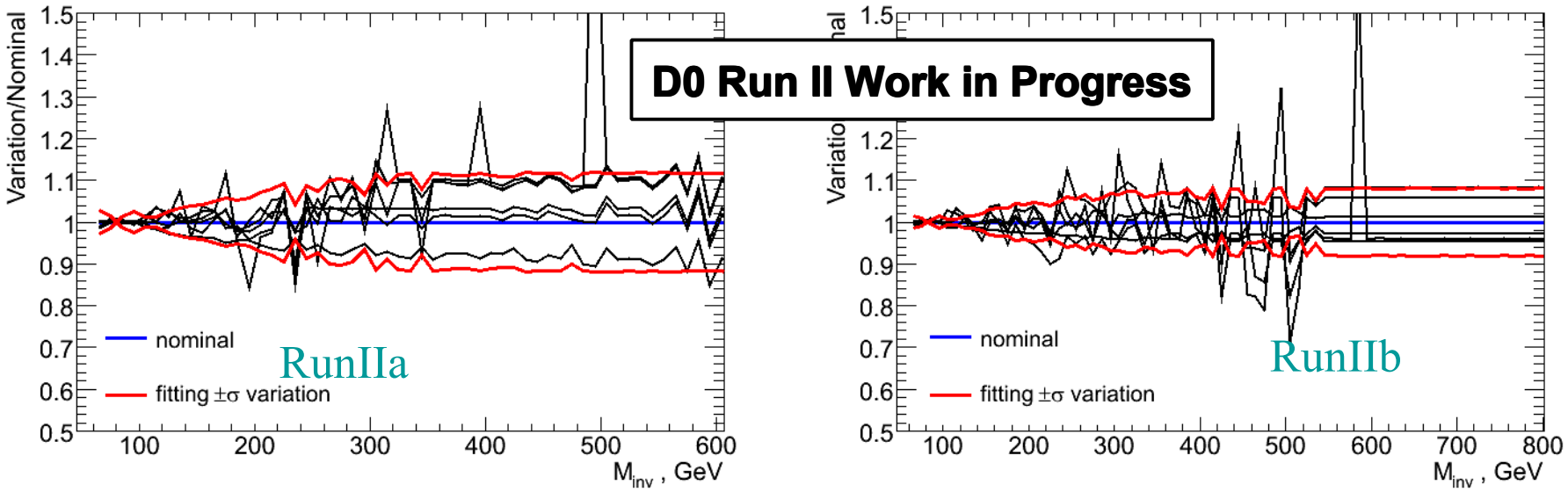

variation of total background w.r.t to the nominal one

1. The fitting uncertainty on the total background is denoted as the red curves on the plots.
2. Effect of instru background variations is covered by the fitting uncertainty.
3. A mass dependent systematic uncertainty is adopted in the limit calculation.